이학박사 학위논문

Large-scale brain networks in resting-state underlying individual differences on response inhibition

반응 억제의 개인차와 관련한 대규모 휴지기 뇌네트워크의 특성

2020년 8월

서울대학교 대학원

협동과정 인지과학 전공

허 영 민

Large-scale brain networks in resting-state underlying individual differences on response inhibition

지도 교수 이 동 수

이 논문을 이학박사 학위논문으로 제출함
2020년 4월

서울대학교 대학원
협동과정 인지과학 전공
허 영 민

허영민의 이학박사 학위논문을 인준함
2020년 8월

위 원 장 _____ 권 준 수 _____ (인)

부위원장 _____ 이 동 수 _____ (인)

위 원 _____ 김 준 식 _____ (인)

위 원 _____ 강 혜 진 _____ (인)

위 원 _____ 하 승 균 _____ (인)

ABSTRACT

Large-scale brain networks in resting-state underlying individual differences on response inhibition

Youngmin Huh

Interdisciplinary Program in Cognitive Science

The Graduate School

Seoul National University

Response inhibition is one of the essential cognitive functions and suppresses inappropriate responses for goal-directed behavior. When a brain is cognitively engaged, it enters a cognitive state that task-positive regions are activated, and the default mode network is deactivated (DMN). In contrast, DMN is activated, and task-positive regions are deactivated at rest. The transition between the states is important for the cognitive function, and recent studies have found that the salience network (SN) plays a crucial role in detecting and processing a salient signal and suppressing DMN at rest. It can be assumed that there exists optimized connectivity to perform response inhibition successfully and that it will also appear in resting-state requiring no cognitive effort. It was hypothesized that lower functional connectivity within SN and higher

functional connectivity within DMN and greater anti-correlation between then is related to better response inhibition.

The response inhibition of individuals was measured by the stop-signal task and the Stroop task. The correlation between intra-/inter-component functional connectivity derived from independent component analysis with dual regression and task performances were examined to test the hypothesis. The intra-/inter-component structural connectivity analysis using diffusion tensor imaging was conducted to provide a deeper understanding of functional connectivity. Topological characteristics of inter-component functional connectivity were also examined using the minimum spanning tree (MST) of each individual to provide a heuristic insight from the topological view.

The results indicate that the functional connectivity within SN, but not DMN components, and the functional and structural connectivity between SN and DMN components are critical to elucidate individual differences in response inhibition. Higher structural connectivity but low functional connectivity of SN at rest was an important feature for superior response inhibition. The stronger structural connectivity and stronger anti-correlation between SN and DMN components were also indicative of better response inhibition. MST of a subject with the best performance showed direct connections between SN and anterior DMN/pDMN, whereas the MST of the one with the worst performance does not. These intra-/inter components connectivities reflect the organization of the brain that enables competent response inhibition and account for individual differences.

This study might suggest that the individual's characteristics of

large-scale network components at rest provide evidence to illustrate response inhibition of an individual without any experimental scan.

Keywords: response inhibition, large-scale network, resting-state functional magnetic resonance imaging, diffusion tensor imaging, brain connectivity, minimum spanning tree

Student Number: 2014-30038

CONTENTS

List of Figures

List of Tables

1. Introduction

1.1. Response inhibition and its neural correlates

Cognitive control is the ability to coordinate goal-directed thoughts and actions, and researchers regarded it as a marker that could explain mechanisms of individual differences in cognitive function (Lee et al., 2015; Nigg et al., 2006; Unsworth et al., 2009). Response inhibition implies behavior that suppresses actions that are inappropriate for the context, and it is one of the most critical components of cognitive control (Bunge et al., 2002). Various tasks, including the Stop-signal task (SST) and the Stroop task, have been developed to assess response inhibition (Friedman et al., 2004; Logan et al., 1984; MacLeod et al., 2000; Stroop, 1935).

1.1.1. Cognitive tasks to measure response inhibition

Response inhibition suppresses a response that is not required in a given context. The SST and the Stroop task are both commonly used to measure response inhibition (Friedman et al., 2004). They instruct not to respond to the prepotent stimuli but to less dominant ones.

In the SST, subjects were instructed to perform a primary task, which is a simple response selection task, and a stop signal is presented occasionally during a trial of the primary task. Previous studies reported that the SST is very sensitive to measure response inhibition than other tasks, e.g., Go/No-go task, Flanker task (Gauggel et al., 2004). In the Stroop task, subjects are told to report

the color of the ink printed, not the meaning of the word. In general, language processing is more dominant than color processing; hence, the task assesses response inhibition (MacLeod et al., 2000).

1.1.2. The neural correlates of response inhibition

Early studies proposed that specific brain region and its connection supports discrete cognitive function (Hampshire et al., 2015). Based on behavioral measures, investigations have found candidate regions of response inhibition, including right inferior frontal gyrus (rIFG), anterior insula (aINS), pre-supplementary area (preSMA), and cortico-striatal-thalamic-cortical loop (CSTC loop) with subthalamic nucleus (STN). Aron suggested that rIFG is the core region that "brakes" the response, and signals from rIFG is sent to the other areas for further processes (Aron, 2007; Aron et al., 2003; Aron et al., 2004, 2014; Chikazoe et al., 2007). The increased activation in aINS was also observed when healthy subjects cancel their response during the task (Rubia et al., 2001).

Contrary to the traditional view that response inhibition arises from a specific brain region, recent studies proposed a globalist view that some distributed brain regions are involved in diverse cognitively-demanding tasks (Erika-Florence et al., 2014; Hampshire et al., 2015). Given that various cortical and subcortical regions were reported to be involved in response inhibition, investigations on large-scale networks may provide a system-level understanding to clarify the neural correlates (Zhang et al., 2017). For example, the salience network is one of the most well-known large-scale networks and

includes aINS and STN, reported in task-based fMRI studies of response inhibition (Aron et al., 2006; Swick et al., 2011). Therefore, not a specific region, but large-scale networks consist of distributed brain regions were investigated in this study.

1.1.3. Response inhibition and resting-state brain

The traditional task-based fMRI has been widely used to investigate various cognitive functions, but the finding may vary depending on the experimental design and stimulus modality (Bennett et al., 2013; Gielen et al., 2018). In contrast, resting-state fMRI (rs-fMRI) focuses on the ongoing spontaneous fluctuation, that covers the entire repertoire of the brain network that reflects active brain, which can be observed by task-based fMRI (Douaud et al., 2015; Fox et al., 2010; Welvaert et al., 2013). Therefore, it is expected that rs-fMRI data analysis would reveal the robust baseline functional connectivity that underlies task-induced state and cognitive function.

In recent years, rs-fMRI studies have emerged as a promising tool to uncover intrinsic connectivity that subserves cognition and behavior (Keller et al., 2015; Kong et al., 2019; Sala-Llonch et al., 2012). Previous studies have shown that intrinsic neural circuitry is related to development, aging, and individual differences in cognitive functions (Amer et al., 2016; Barber et al., 2013; Chai et al., 2014).

Response inhibition is involved in a wide range of cognitive processing, and the deficit of response inhibition is related to diverse psychiatric diseases with maladaptive behaviors: Attention-

deficit/hyperactivity disorde (ADHD), conduct disorder, and addictive disorders (Lawrence et al., 2009; Nigg et al., 2006; Slaats-Willemse et al., 2003; van der Meer et al., 2004). Since response inhibition is associated with broad classes of cognitive processing (Bechara et al., 2004; Fichten et al., 1986; Roberts et al., 1994), it is assumed that the brain at rest, the basic circuit underlying task-state, will also reflect individual differences in response inhibition in this study.

1.2. Investigations on large-scale networks underlying response inhibition

1.2.1. Resting-state networks and response inhibition

The resting-state networks are the most well-known large-scale networks consist of distributed brain regions that work together. Resting-state networks have been identified with a number of methods, such as Independent component analysis (ICA). Researchers reported few networks, including default mode network (DMN), salience network (SN), and central executive network (CEN), that are robust and reproducible (Damoiseaux et al., 2006). Moreover, recent findings implicated that resting-state networks are potential biomarkers for psychiatric disease that involves cognitive impairments (Di et al., 2014; Menon, 2011). For example, the disrupted functional connectivity within DMN was found in patients with Alzheimer's disease (AD), and it showed a significant relationship with the hallmark of AD, the beta-amyloid

deposition (Elman et al., 2014). Numerous studies have investigated the resting-state of the brain, and it was expected to be one of the most convenient and efficient ways to understand brain functions.

When a brain is engaged in a task that requires cognitive demands, brain regions related to the cognitive function are activated, and the DMN is deactivated. In contrast, task-positive regions are deactivated, and the DMN is activated at rest. Previous studies found that states switch to respond to cognitive demand (Nour et al., 2019). DMN shows deactivation during the task, and the magnitude of the change was related to cognitive load (Mckiernan et al., 2003; Sambataro et al., 2010). Moreover, anti-correlation between SN and DMN is observed in both the tasking-state and resting-state of the brain due to their opposing properties (Buckner et al., 2008; Chai et al., 2014).

SN is known to be essential to change states since the SN interacts with DMN and CEN. The causal influence from SN to DMN is related to better performances at a task that requires top-down regulation of internal noise (Wen et al., 2013). Due to the role of SN that interacts with other networks, SN is considered to be a modulator that switches DMN and CEN depending on the cognitive demands. SN is involved not only in top-down but also in bottom-up mechanisms and plays an important role in salient stimulus processing (Menon, 2015; Menon et al., 2010). The aINS receives external sensory information via posterior insula and internal-oriented information. The aINS also interacts with various cortical regions to mediate top-down processing.

The response inhibition requires to detect proper stimulus that provokes suppression of an action. Information is abundant around, and the

detection of an appropriate stimulus is important for response inhibition. The SN engages in detecting salient stimuli and directing attention to an external stimulus, not toward the internal process, to achieve successful inhibitory control (Menon et al., 2010). Thus, it was inferred that SN and DMN and the functional connectivity between them are related to response inhibition.

1.2.2. Structural connectivity

There has been an ongoing debate over the relationship between brain structure and function. Previously, significant correlations between structural connectivity and functional connectivity were observed (Honey et al., 2009; Koch et al., 2002), but it is challenging to set their straightforward correspondence. The cases of functionally connected but no anatomical pathway between regions are fairly found (Koch et al., 2002), and the heterogeneity of structural and functional connectivity has been discussed. The structural connectivity tends to be spatially constrained (Bullmore et al., 2012), while functional connectivity arises from distributed brain regions (Thomas Yeo et al., 2011). However, the importance of structural links is agreed upon, and the links may underlie as a backbone for functional connectivity.

In this study, the structural connectivity of the resting-state network has been investigated for a profound understanding of functional connectivity. Previous studies have shown that structural connectivity is important to resting-state networks and also contributes to functional connectivity and cognitive functions. The structural connectivity of the cingulum tract connecting the precuneus/posterior cingulate cortex and medial frontal cortex, the core regions

of DMN, was related to FC between them (van den Heuvel et al., 2008). The inferior occipitofrontal fasciculus and the uncinate fasciculus pass through insula (Wang et al., 2011), and they were associated with response inhibition and developmental disorders with inhibition impairment (Olson et al., 2015; Rollans et al., 2018).

In this study, structural connectivity analysis was conducted to support and provide a deeper understanding of functional connectivity underlying response inhibition.

1.2.3. Topological characteristics

Functional coupling between target nodes is one of the most critical features to characterize neural substrates. It investigates pairwise relationships between nodes in a traditional way. However, the topological data analysis, which has risen with recent advances, enabled interpretation from functional connectivity in a topological perspective (Lee et al., 2011a; Lee et al., 2011b). A brain is assumed as a small-world network consisting of nodes, the brain regions, and edges connecting them to investigate topological characteristics. It provides an insight in terms of a wholly connected structure of the system, not a pairwise relationship (Giusti et al., 2016; Lee et al., 2011a; Lee et al., 2011b). In recent years, topological data analysis plays an important role in neuroscience, and it has been used to find a biomarker for a specific disease (Ha et al., 2020; Lee et al., 2019).

In this study, a minimum spanning tree (MST) of each subject was estimated and displayed to visualize the topological characteristics of the large-

scale networks underlying response inhibition at rest. It reflects not only the pairwise functional connectivity but also the whole system connected from a topological view, providing profound knowledge with the widened scope of functional connectivity.

1.2.4. The aim of the present study

In this study, large-scale networks at rest were investigated to figure out neural correlates of individual differences in response inhibition. It was expected that the intrinsic circuits at rest would reflect task-induced state with cognitive demands, and therefore would provide a system-level understanding encompassing task-based studies. The structural connectivity was also examined to give a deeper understanding of the nature of functional connectivity.

It was hypothesized that low functional connectivity of SN and high functional connectivity of DMN and high anti-correlation between them at rest to be associated with better response inhibition. The analyses were conducted as follows to test this hypothesis. First, the functional connectivity within a resting-state network and between two resting-state networks were tested for correlations with response inhibition. Second, structural connectivity was examined to provide a further understanding of functional connectivity. Finally, each individual's MST was estimated to provide an insight into the relationship between SN and DMN from the topological view.

2. Methods

2.1. Subjects

For the study, 22 healthy and right-handed adults without any psychiatric disease were recruited (Table 1). They underwent the Korean version of screening tests: CES-D (Center for Epidemiologic Studies Depression Scale) (Hahn, 1982), MMSE (Mini-Mental State Examination) (Kang et al., 1997), STAI-X (State-Trait Anxiety Inventory) (Kim et al., 1978). Subjects who meet screening criteria were included for the study (CES-D < 16, STAI < 50, MMSE $\geq$ 28). Two subjects were excluded in whole analysis: one subject suspected of the arachnoid cyst; one subject with missing behavioral data. One more subject was excluded only in diffusion tensor imaging (DTI) analysis due to technical problems on DTI data acquisition. In total, rs-fMRI data of 20 subjects (male = 4; female = 16, mean age = 26.45 ± 5.20, mean education year = 15.55 ± 2.77) and DTI data of 19 subjects (male = 4; female = 15, mean age = 25.89 ± 4.72, mean education year = 15.58 ± 2.83) were included for analysis. The study was approved by the Institutional Review Board of Seoul National University Hospital (IRB No. 1312-121-545), and the study complied with the tenets of the Declaration of Helsinki. Informed consent was obtained from all individual subjects recruited, and a hard copy was given to all subjects.

Table 1. Demographic information of subjects. The mean and standard deviation of variables for rs-fMRI (n=20) and DTI (n=19) analysis was presented. One subject was excluded from DTI analysis.

Variable	Modality	
	rs-fMRI (n = 20)	DTI (n = 19)
Age (years):		
Mean	26.45	25.89
SD	5.20	4.72
Gender:		
Male	4	4
Female	16	15
Education (years):		
Mean	15.55	15.58
SD	2.77	2.83
MMSE		
Mean	29.50	29.47
SD	0.59	0.60
CES-D		
Mean	8.70	8.58
SD	3.72	3.77
STAI-X		
Mean	34.60	34.74
SD	6.18	6.31

rs-fMRI: resting-state functional magnetic resonance imaging, DTI: diffusion tensor imaging, CES-D: The Center for Epidemiologic Studies-Depression Scale, STAI-X: State-Trait Anxiety Inventory.

2.2. Behavioral tasks to assess response inhibition

Response inhibition was estimated using the stop-signal task (SST) (Logan et al., 1984) and the Stroop task (Stroop, 1935) (Figure 1). The tasks were conducted to the subjects using Inquisit 4 (https://www.millisecond.com/).

In SST, stop-signal reaction time (SSRT) was measured to assess response inhibition. An arrow pointing left or a right was randomly shown on the screen, and subjects were told to press a corresponding button in a go trial (i.e., primary task) (Figure 1 (a)). In some trials, a beep sound representing a stop signal comes after the arrow stimulus after a stop-signal delay (SSD) (stop trial) (Figure 1 (b). Subjects were told to withhold the response when they listen to a stop signal. SSRT is a duration of the stop process, and the higher SSRT indicates poorer response inhibition.

The successful inhibition does not emit any behavioral output, so the SSRT can be estimated as follows. The distribution of the response time (RT) of the primary task trials, i.e., go trials without stop-signal, represents the finishing time of the go-process. Assuming the independence of Go and Stop processes, the finishing time of Stop-process bisects the RT distribution: p(respond|signal), p(inhibit|signal). The task dynamically adjusts the SSD depending on an individual's performance of the previous trial. The SSD is set to 250ms at the first trial, and increases by 50ms after successful inhibitory trial and decreases by 50ms after the subject fails to inhibit. The procedure stops when a subject successfully inhibit half of the trial with the stop signal, i.e., p(inhibit|signal)=.5. The 50^{th} percentile of rank-ordered RT distribution is the point that bisects the distribution, and it is called the internal response to the

stop signal. An individual cannot inhibit the response if the RT is smaller than an internal response to the stop signal on stop trials. The SSRT can be calculated by subtracting mean SSD from mean RT.

In the Stroop task, three types of stimuli were presented during the task. A colored rectangle (control condition) (Figure 1 (c)) or a word representing the name of the color (incongruent/congruent condition) was displayed on the screen. The name of the color was presented under the two conditions: in the same ink color as it spelled out (congruent condition: 'Green' in green ink) (Figure 1 (a)) or in different ink colors (incongruent condition: 'Green' in red ink) (Figure 1 (b)). Subjects were instructed to choose the color of ink, not the name of the color spelled out, by pressing the corresponding keyboard. The differences between three conditions were assessed using a one-way analysis of variance (ANOVA) with post hoc Bonferroni tests to correct for multiple comparisons. The error rate for the incongruent condition was used for analysis as a measure of response inhibition. A higher error rate shows poorer response inhibition of an individual.

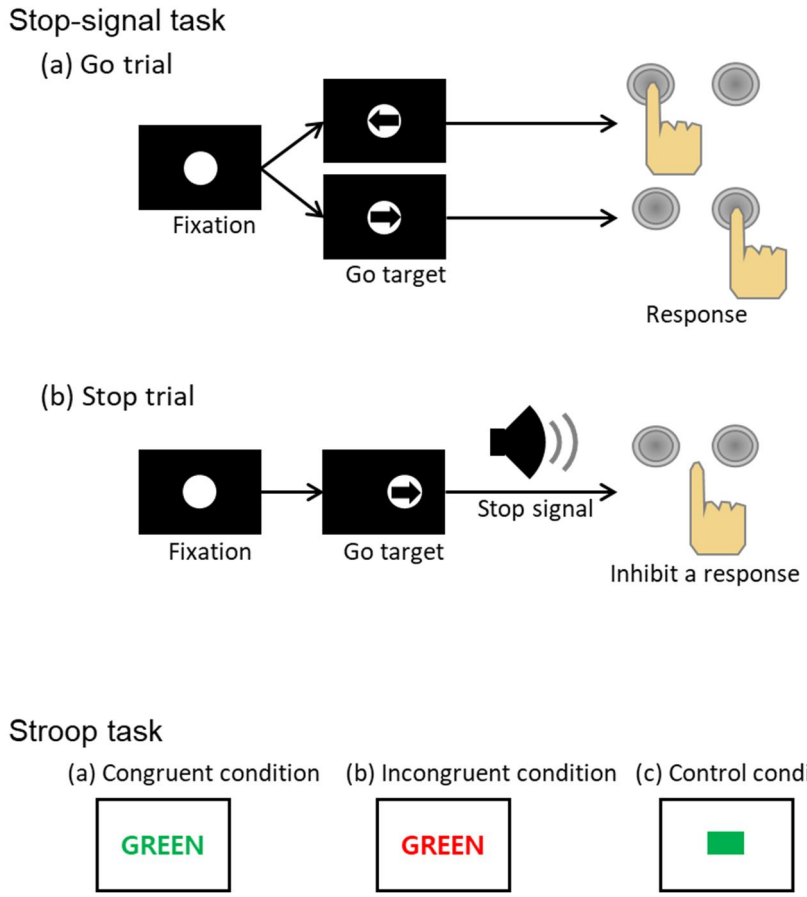

Figure 1. Two behavioral tasks to assess response inhibition. (Top) In the Stop-signal task (SST), subjects were instructed to push a button according to the stimulus shown on the screen (a). The stop trial is randomly presented, and subjects were told to withhold their response when the stop signal is given (b). (Bottom) There are three kinds of stimuli in the Stroop task. Subjects were shown a word representing a color, which is written in (a) identical ink color with the word, or (b) incongruent ink color with the word (ex. the word 'green' written in red ink). (c) A colored rectangle was displayed in the control condition. Subjects were instructed to press a button which represents the color of the ink of the stimulus, not the meaning of the word.

2.3. Brain imaging data acquisition and preprocessing

2.3.1. Resting-state fMRI

Subjects were scanned on a 3-T scanner (Magnetom Biograph mMR, Siemens Healthcare, Erlangen, Germany) with 16–channel head coil. Spoiled gradient echo (SPGR) T1-weighted images were obtained with following parameters: repetition time (TR) = 1679ms, echo time (TE) = 1.89ms, flip angle = 9°, field-of-view (FOV) = 250 × 250mm^2, matrix size = 256 × 256, 208 sagittal slices of 1mm thickness, voxel size = 1.0 × 1.0 × 1.0mm^3. The rs-fMRI data were collected with parameters as below: TR = 3000ms, TE = 30ms, flip angle = 90°, FOV = 240 × 240mm, matrix size 128 × 128, 45 axial slices with 3mm thickness, voxel size = 1.9 × 1.9 × 3.0mm^3, resulting 180 volumes. Subjects were given instructions not to sleep and not to think of anything specific during scanning with their eyes closed.

Statistical Parametric Mapping (SPM, www.fil.ion.ucl.ac.uk/spm/) was used for resting-state data preprocessing. After discarding five volumes, imaging data were inspected for noisy slices and repaired by ArtRepair Software (https://cibsr.stanford.edu/tools/human-brain-project/artrepair-software.html) (Mazaika et al., 2005). Data quality was checked manually after the repair, and subjects with mean frame-wise displacement < 0.2mm were included in the study (Power et al., 2012). Each subject's rs-fMRI data were corrected for motion artifacts after slice timing correction. Images were coregistered to anatomical T1 weighted images and normalized to MNI space. Next, they underwent smoothing, and the intensity of gray matter was

normalized to a whole-brain median of 1000 (Patel et al., 2014). Wavelet despiking was performed to denoise the data (Patel et al., 2016), then white matter, CSF, 6 motion parameters were regressed out, and bandpass filtering (0.01Hz-0.1Hz) was done.

2.3.2. Diffusion tensor imaging

DTI data were obtained with TR = 9500ms, TE = 92ms, FOV = 230 × 230mm^2, matrix size 114 × 114, 66 axial slices with 2mm thickness, voxel size = 2.0 × 2.0 × 2.0mm^3, b-value = 1,000sec/mm^2, 60 gradient directions and 8 reference images (b = 0). DTI images were preprocessed using FMRIB's Diffusion Tool (FDT, http://www.fmrib.ox.ac.uk/fsl) and Diffusion Toolkit (DTK, http://trackvis.org/dtk/). Data were corrected for eddy current distortion and subject movements (Andersson et al., 2016). Tensor reconstruction calculating eigenvectors of each voxel was performed using extracted gradient direction information. The preprocessed data were manually inspected for any noise or abnormal motion, and whole-brain fiber tracking was implemented with an interpolated streamline propagation algorithm, which is a modified Fiber Assignment Continuous Tracking (FACT) algorithm (Conturo et al., 1999; Mori et al., 1999). The algorithm builds streamlines by tracing the pathways from a seed region by following the diffusion tensor's principal eigenvectors from one voxel to the next voxel. The voxels with fractional anisotropy (FA) values larger than 0.2 were included for fiber tracking, and ten seeds per voxel were set to reconstruct streamlines starting from the random location of a voxel. If a turning angle between two voxels is greater than 35°, the tracking procedure

stopped.

2.4. Resting-state networks and functional connectivity analysis

2.4.1. Group independent component analysis to identify resting-state networks

Independent component analysis (ICA) was carried out using Multivariate Exploratory Linear Decomposition into Independent Components (MELODIC) to figure out independent components (IC's), i.e., resting-state networks (Beckmann et al., 2009) (Figure 2, (a)). The ICA finds projections of maximal independence. According to the central limit theory, random mixing of random variables results in Gaussian. Conversely, it is possible to find the independent component by estimate non-Gaussianity.

$$Y = XB + E \quad (1)$$

Y is concatenated data of all 20 subjects in standard space, which was used for estimation resulting in 25 independent components, B. X contains the time-course of components, and E denotes Gaussian noise. Twelve network components, the group IC maps, were identified for the analysis: (a) anterior default mode network (aDMN), (b) posterior DMN (pDMN), (c) Salience network (SN), (d) left CEN (Lt CEN), (e) right CEN (Rt CEN), (f) Dorsal attention network (DAN), (g) Ventral attention network (VAN), (h) medial Visual network (medVN), (i) lateral VN (latVN), (j) primary VN (priVN), (k)

Sensorimotor network (SMN), (l) Basal ganglia and cerebellar network (BGCN) (Figure 3).

2.4.2. Dual regression to obtain subject-specific data of components

Dual regression was performed to calculate subject-specific spatial maps that include parameter estimates, and the time-courses for each component (Beckmann et al., 2009; Filippini et al., 2009) (Figure 2, (b)). Firstly, in the spatial regression, group IC spatial maps were regressed to each subject's four-dimensional (4D) dataset to estimate subject-specific time-courses for each component:

$$\mathrm{Y} = S_g B_{TC} + E_1 \quad (2)$$

Y denotes dataset of the subject which is reorganized into two-dimensional data matrix (N voxels $\times$ T time points), and S_g is group IC maps obtained from group ICA and is identically assigned to all subjects. B_{TC} is the time course of the components, one for each component. E_1 denotes the matrix of errors. Next, in the temporal regression, the temporal information, which is the output from the first stage was regressed to each subject's preprocessed dataset to estimate the subject-specific set of spatial information, i.e., parameter estimation maps:

$$\mathrm{Y} = B_{TC} B_{SM} + E_2 \quad (3)$$

The B_{SM} consist of spatial maps of the subject. The spatial map contains parameter estimates (beta values) per voxel, and they represent the functional connectivity of a given component. The spatial maps were obtained for each

corresponding component.

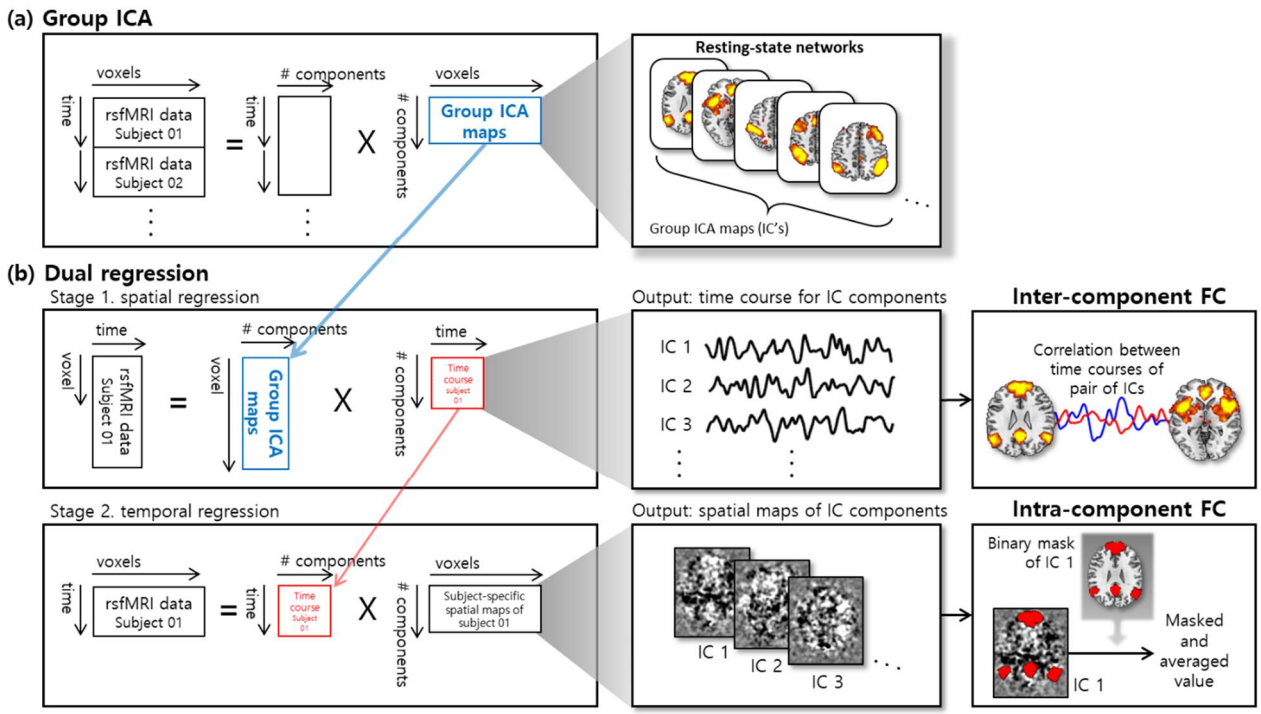

Figure 2. The workflow of calculating intra-component functional connectivity (FC) and inter-component FC. (a) The group independent component analysis (ICA) was conducted to extract resting-state networks. (b) In the first stage, group IC maps were entered as a regressor in spatial regression, and a subject-specific time course for each IC map, i.e., resting-state networks were obtained. The correlation coefficient between time courses of two components was calculated as the inter-component functional connectivity (FC) of an individual. The output from stage 1, the time course, was entered as a regressor in stage 2 temporal regression. Subject-specific spatial maps, which are parameter estimation maps consist of beta values, were obtained for each component and masked with binarized group IC maps. The mean of masked values was calculated to examine intra-component FC.

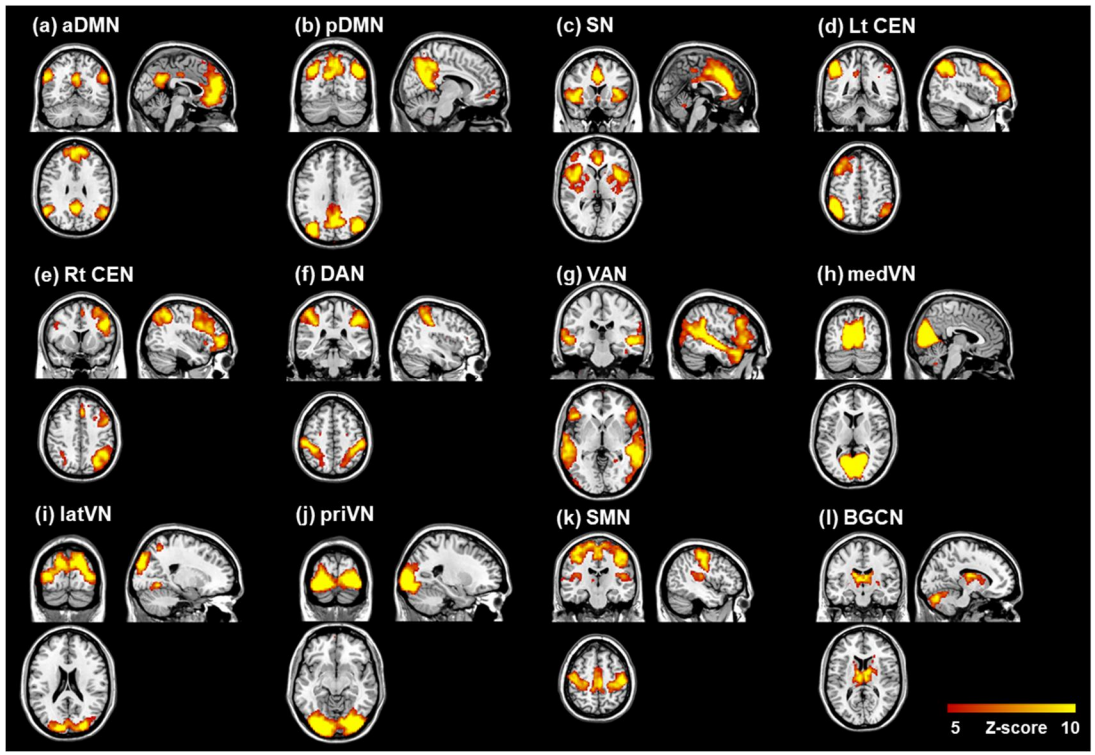

Figure 3. The resting-state networks included in this study. Twelve components were obtained by independent component analysis (ICA), and included in the analysis: (a) anterior default Mode Network (aDMN), (b) posterior DMN (pDMN), (c) Salience Network (SN), (d) left Central Executive Network (Lt CEN), (e) right Central Executive Network (Rt CEN), (f) Dorsal Attention Network (DAN), (g) Ventral Attention Network (VAN), (h) medial Visual Network (medVN), (i) lateral Visual Network (latVN), (j) primary Visual Network (priVN), (k) Sensorimotor Network (SMN), (l) Basal Ganglia and Cerebellar Network (BGCN).

2.4.3. Estimation of subject-specific intra-/inter-component functional connectivity

Subject-specific time-courses and spatial maps for each component were used for analysis. A mask image was generated by thresholding a group IC map (Z>5) and applied to a subject-specific spatial map, the parameter estimation map. Extracted parameter estimation values were averaged to assess intra-component functional connectivity. The intra-component represents the association between a single subject-specific time-course of a component obtained by the first stage in dual regression, and time-courses of the voxels composing a component. It shows large value when voxels from a subject-specific spatial map of a component are highly correlated to a subject-specific time-course of a component (Elman et al., 2014; Rolinski et al., 2015; van Duijvenvoorde et al., 2016).

The correlation coefficients between the time-courses of the pair of components were calculated to examine inter-component functional connectivity. The intra-/inter component FC were tested for correlation with the performance of each task, respectively, that measured response inhibition. The age and gender effects were regressed out.

2.5. Structural connectivity analysis

2.5.1. Structural connectivity and response inhibition

Binary mask images using IC maps (Z > 5) were warped into an individual

native space, and they were used as ROI to examine structural connectivity. The streamlines representing white matter were reconstructed by the tractography technique. The streamlines that both endpoints belong to one network component were classified to estimate intra-component structural connectivity. The mean FA of all voxels of which the streamlines pass was calculated to assess the intra-component structural connectivity. The voxels with their FA higher than 0.2 are included for the analysis to exclude gray matter and cerebrospinal fluid (Jones, 2010). Next, the streamlines connecting two components were identified to estimate inter-component structural connectivity. The mean FA of all voxels of which classified streamlines pass was calculated as inter-component structural connectivity (Figure. 4). Overlapping areas of network components were excluded in the analysis.

In an analysis that investigated intra-/inter-component structural connectivity, components, and edges showing significant correlations with response inhibition in functional connectivity analysis were included. Four components for intra-component SC and thirteen pairs of inter-component structural connectivity were examined for correlations with task performances representing response inhibition in this analysis. The age and gender effects were regressed out.

2.5.2. Relationship between functional connectivity and structural connectivity

In inter-component functional connectivity analysis, thirteen edges that showed significant correlations with response inhibition were found. The structural

connectivity of thirteen edges were tested for correlation with response inhibition, and one edge showed significant correlations with SSRT in both functional and structural analysis: connectivity between SN and pDMN. In this analysis, the correlation between functional and structural connectivity between SN and pDMN was examined.

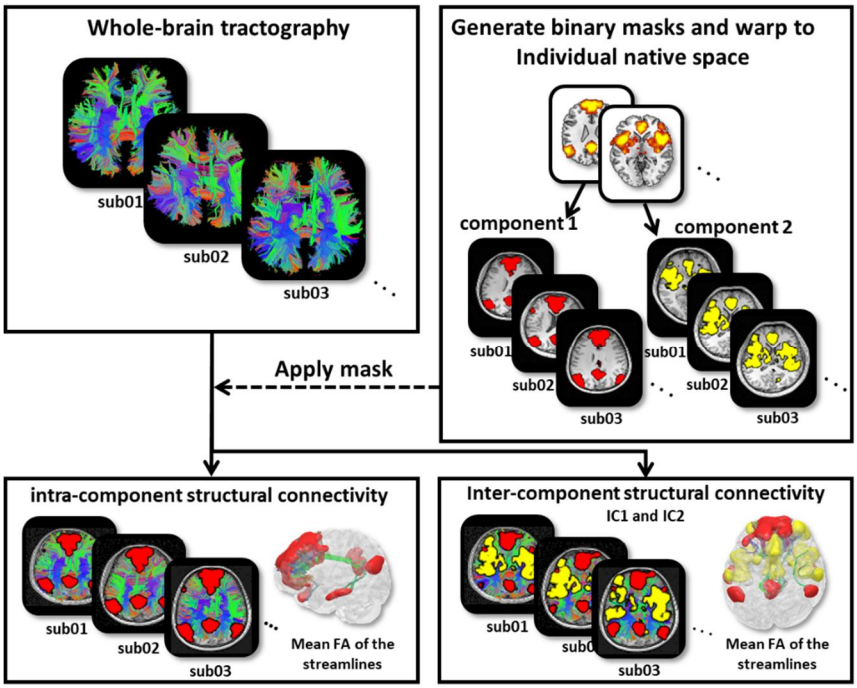

Figure 4. The workflow to calculate intra-component structural connectivity (SC) and inter-component SC. The whole-brain tractography was implemented in individual native space. The binary masks of group IC maps were generated, and they were warped from standard space to individual native space. The streamlines that both endpoints are located in a component were classified, and their mean fractional anisotropy (FA) was calculated as an intra-component SC. The streamlines connecting pairs of components were also identified, and their mean FA was estimated as the inter-component SC.

2.6. Topological data analysis

2.6.1. Minimum spanning tree

To compare characteristics of topological structure associated better and poor performance of response inhibition, the MST was calculated and displayed. MST is a tree whose sum of the edge weight is minimum when all the nodes are connected with the least number of edges.

Subjects were ranked in order of good performance of each task to identify one subject who performed the best and one who performed the worst. The sum of the ranks of two tasks was used to assess performance and to identify the best and the worst performers. Subject #5 was one whose performance was the best, and the performances of both tasks were in the top 10% (SSRT = 117ms, the error rate of the Stroop task = 3.75%). The performances of subject #19 were in the bottom 10% in both tasks and identified to be the worst (SSRT = 351ms, the error rate of the Stroop task = 15%). Besides, the MSTs of all subjects were estimated to investigate the individual differences in the topological backbone structure.

The connectivity matrix that consists of absolute values of negative correlation coefficients was used to estimate an MST. The distance matrix for each subject was calculated as follows:

$$\mathbf{d}(x_i, x_j) = \sqrt{\mathbf{1} - |corr(x_i, x_j)|} \quad (4)$$

MST of each group was obtained by Kruskal's algorithm (Kruskal,

1956). Let G be a connected graph with node set V, and let w be the weight of edge set, E. The edges of G were sorted in ascending order according to weight. The algorithm assumes that $G = (V, E, w)$ is a weighted undirected graph with m, the number of nodes, and n, the number of edges. Initially, there is no edge connected in G. The edge with the smallest weight is added to G, and it was checked if G forms a cycle. If a cycle is formed, the edge is discarded, and otherwise, included. The procedure that adds an edge is repeated until there are $(m - 1)$ edges in the tree. In this analysis, twelve nodes were included, and MST with eleven edges was estimated for each subject.

3. Results

3.1. The performances of behavioral tasks

Twenty subjects underwent two tasks: the SST and the Stroop task. The SSRT ranged from 103.83ms to 351.46ms across subjects, and the average SSRT was 195.71ms (± 58.80ms). The error rates of three conditions in the Stroop task were measured: The congruent condition (1.49 ± 2.71%), the incongruent condition (7.03 ± 5.77%), and the control condition (0.74 ± 1.87%) (Table 2). The differences in mean error rates between conditions were found. The error rate of the incongruent condition was significantly higher than the error rates of the congruent condition and control condition ($p < 0.0005$) (Figure 5).

Table 2. The performances of behavioral tasks.

Characteristic	Modality	
	fMRI (N = 20)	DTI (N = 19)
SSRT (ms)		
Mean	195.71	197.14
SD	58.80	59.99
The error rate of the Stroop task (%)		
Congruent condition		
Mean	1.49	1.57
SD	2.71	2.76
Incongruent condition		
Mean	7.03	7.00
SD	5.77	5.92
Control condition		
Mean	0.74	0.78
SD	1.87	1.91

SSRT: Strop-signal reaction time, SD: standard deviation, fMRI: functional resonance imaging, DTI: diffusion tensor imaging

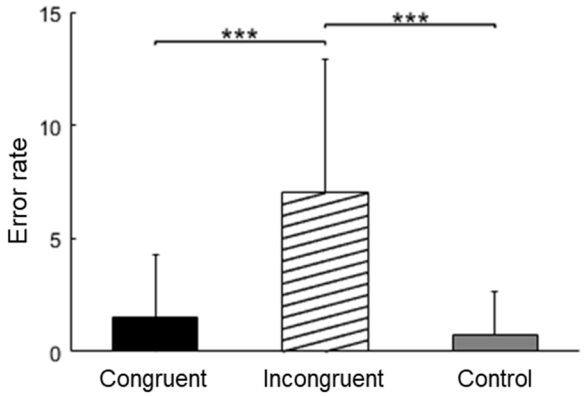

Figure 5. The comparison of error rates between conditions of the Stroop task. There were significant differences in error rates between congruent and incongruent conditions and between incongruent and control conditions ($p < 0.0005$). *** $p < 0.005$.

3.2. Intra-component connectivity and response inhibition

The correlation between intra-component functional connectivity and the performance of response inhibition was examined. The SN was the only component that showed significant correlations with both tasks (Figure 6, Table 3). The functional connectivity within SN was positively correlated to SSRT ($r = 0.60$, $p < 0.01$) and the error rate of incongruent condition of the Stroop task ($r = 0.49$, $p < 0.05$).

The correlation between response inhibition and inter-component structural connectivity was tested as well. The component that showed significant correlations in functional analysis, SN, VAN, latVN, and SMN were included for the analysis. SN was significantly correlated to SSRT ($r = -0.46$, $p < 0.05$) (Figure 7, Table 4).

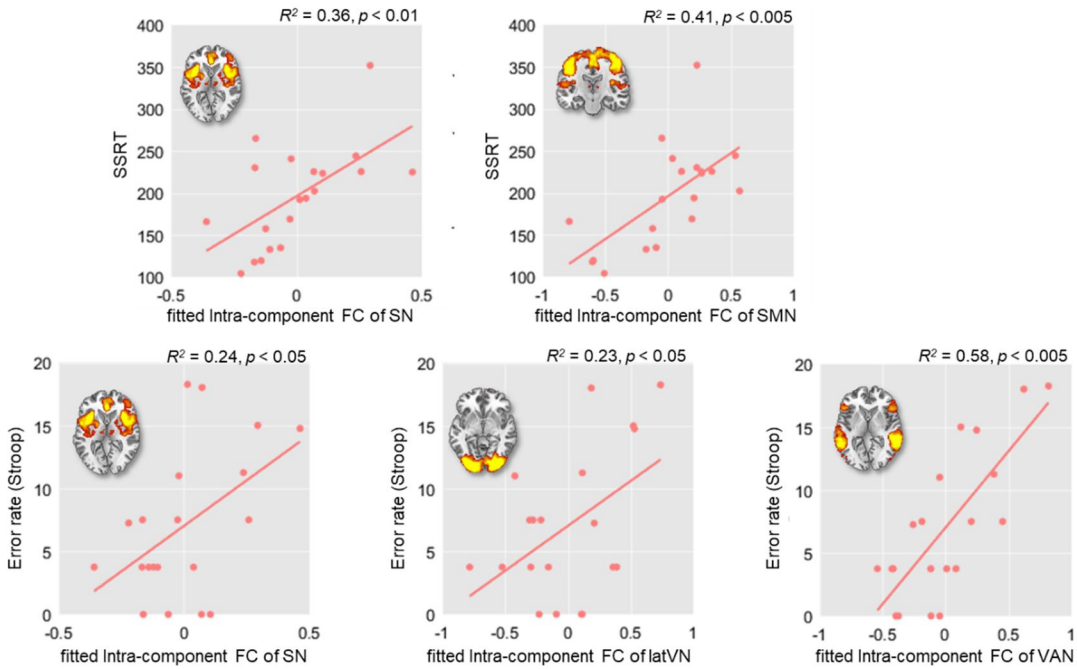

Figure 6. The components that showed significant correlations between their intra-component functional connectivity and behavioral tasks. The intra-component functional connectivity (FC) of SN ($R^2 = 0.36$, $p < 0.01$), SMN ($R^2 = 0.41$, $p < 0.005$) showed significant correlation between strop signal reaction time (SSRT). The error rate of incongruent condition of the Stroop task showed significant positive correlations with intra-component FC of SN ($R^2 = 0.24$, $p < 0.05$), latVN ($R^2 = 0.23$, $p < 0.05$), and VAN ($R^2 = 0.58$, $p < 0.005$).

Table 3. The components that showed significant correlations between their intra-component functional connectivity and behavioral tasks.

Variable (Task)	Resting-state network (component)	*r*	*p*-value (uncorrected)
SSRT			
	SN [a]	0.60	< 0.01
	SMN	0.64	< 0.005
The error rate of the incongruent condition in the Stroop task			
	SN [a]	0.49	< 0.05
	VAN	0.76	< 0.0005
	latVN	0.48	< 0.05

SSRT: Strop-signal reaction time, SN: Salience network, SMN: Sensorimotor network, VAN: Ventral attention network, latVN: lateral visual network. The results that showed significant correlations with both tasks were indicated by [a].

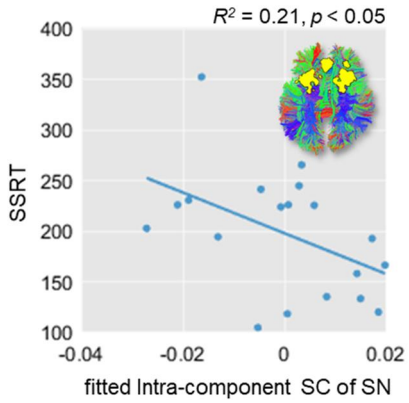

Figure 7. Significant correlations between intra-component structural connectivity (SC) and response inhibition. The significant correlation between the intra-component SC of SN (R^2 = 0.21, p < 0.05) was found.

Table 4. The results that showed a significant correlation between intra-component structural connectivity and behavioral tasks were displayed.

Variable (Task)	Resting-state network (component)	*r*	*p*-value (uncorrected)
SSRT			
	SN	-0.46	< 0.05

SSRT: Strop-signal reaction time, SN: Salience network

3.3. Inter-component connectivity and response inhibition

In the results that tested the correlation between inter-component functional connectivity and the performance of the response inhibition, three pairs were found significant in both tasks: SN-aDMN/pDMN, SN-medVN, and aDMN-SMN (Figure 8). Functional connectivity between SN and pDMN showed a positive correlation with SSRT ($r = 0.47$, $p < 0.05$), and the one between SN and aDMN showed a positive correlation with the performance of the Stroop task ($r = 0.52$, $p < 0.05$). The edges that showed a significant relationship with each task are not identical, but both edges represent the connection between SN and the task-negative component (aDMN and pDMN). The inter-component functional connectivity between SN-medVN and aDMN-SMN showed significant positive correlations with both tasks ($p < 0.05$) (Figure 8, 9, Table 5).

To investigate the relationship between inter-component structural connectivity and response inhibition, the connections that showed significant correlations in functional analysis, the thirteen pairs of components were included for the analysis. In terms of inter-component structural connectivity analysis, lower SSRT was associated with greater inter-component structural connectivity between SN and aDMN/pDMN: SN-aDMN ($r = -0.51$, $p < 0.05$), SN-pDMN ($r = -0.56$, $p < 0.05$) (Figure 10, Table 6). There was no significant relationship between the structural connectivity of targeted edges and the performance of the Stroop task.

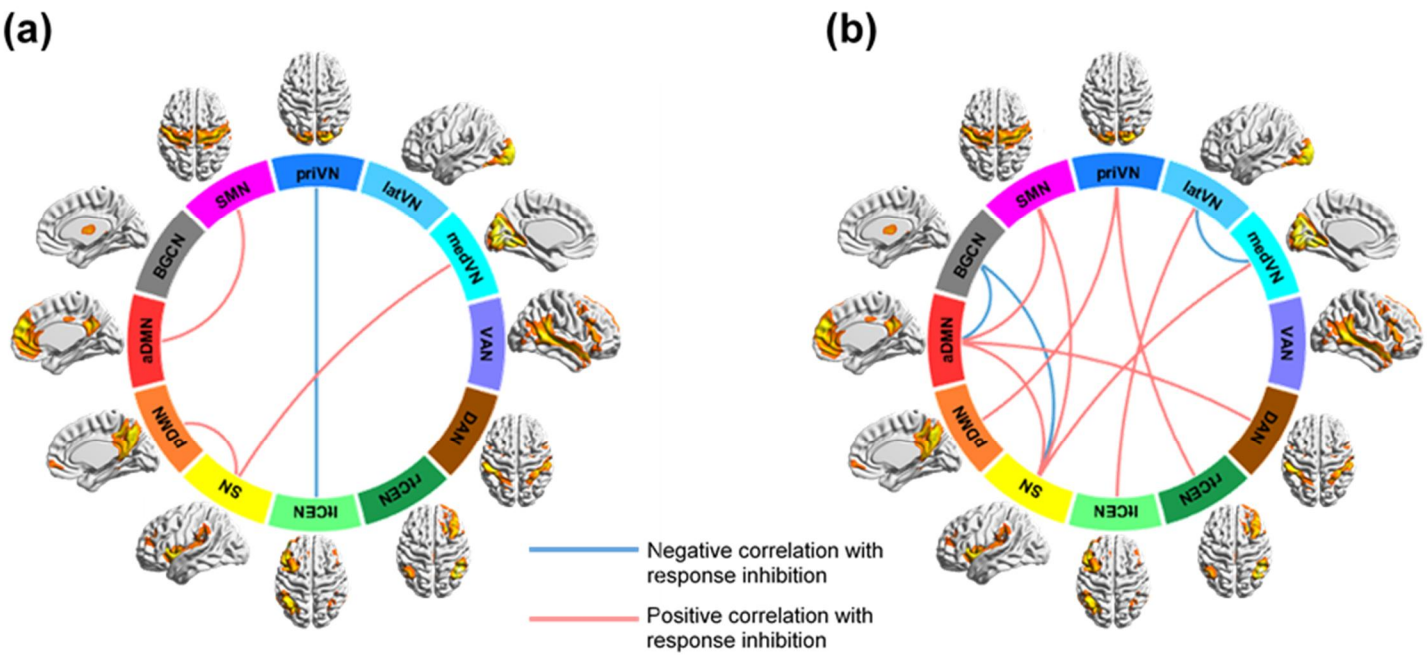

Figure 8. The significant correlations between inter-component functional connectivity (FC) and response inhibition. The correlation between inter-component functional connectivity (FC) and response inhibition was examined, and the significant results ($p < 0.05$) were displayed. (a) The poorer response inhibition, i.e., the longer stop-signal response time (SSTR), was associated with higher FC of SN-pDMN/medVN, aDMN-SMN ($p < 0.05$). The negative correlation between SSRT and inter-component FC between ltCEN and priVN ($p < 0.05$) was found. (b) The poorer performance of the Stroop task was associated with greater functional connectivity between SN and aDMN, between aDMN and task-positive components, between SN and task-positive components, and between task-positive components ($p < 0.05$). The relationships between better response inhibition and the higher FC of BGCN-aDMN/SN, and latVN-medV ($p < 0.05$) were also found.

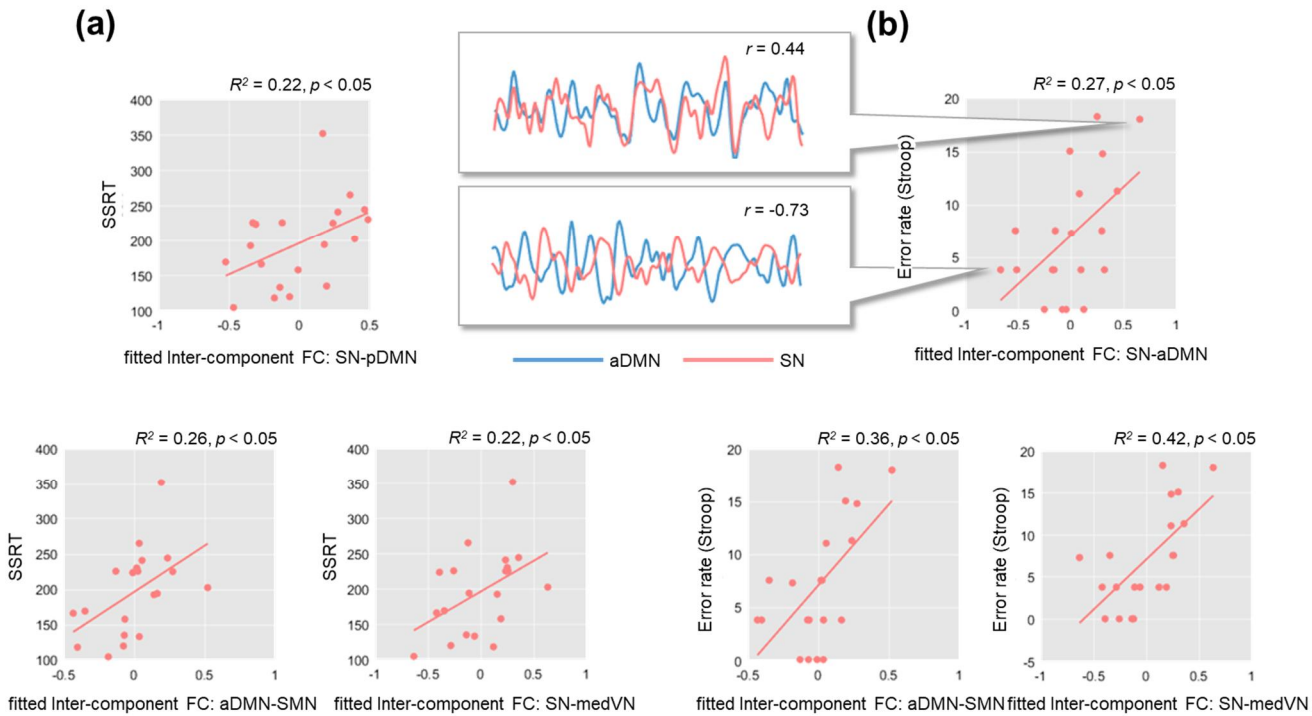

Figure 9. The edges that showed significant correlations with response inhibition in common in both tasks: SN-aDMN/pDMN, aDMN-SMN, SN-medVN. (a) The edges showed positive correlations with (a) SSRT, and (b) the error rate of the Stroop task. The time-courses of SN and aDMN of two subjects who showed low functional connectivity (FC) and high FC were illustrated. The correlation coefficient values between the time-courses of SN and aDMN (r) of two subjects shown in the middle are not regressed out for age and gender effect.

Table 5. The Pair of components that showed significant correlations between their inter-component functional connectivity and behavioral tasks.

Variable (Task)	Pair of components	*r*	*p*-value (uncorrected)
SSRT			
	SN-pDMN	0.47	< 0.05
	SN-medVN [a]	0.46	< 0.05
	aDMN-SMN [a]	0.51	< 0.05
	ltCEN-priVN	-0.50	< 0.05
The error rate of the incongruent condition in the Stroop task			
	SN-aDMN	0.52	< 0.05
	SN-medVN [a]	0.65	< 0.005
	SN-SMN	0.45	< 0.05
	SN-BGCN	-0.49	< 0.05
	aDMN-SMN [a]	0.60	< 0.005
	aDMN-DAN	0.51	< 0.05
	aDMN-BGCN	-0.45	< 0.05
	pDMN-priVN	0.45	< 0.05
	ltCEN-latVN	0.61	< 0.005
	rtCEN-priVN	0.56	< 0.01
	medCN-latVN	-0.73	< 0.0005

SSRT: Strop-signal reaction time, aDMN: anterior default mode network, pDMN: posterior DMN, SN: Salience network, ltCEN: left Central executive network, rtCEN: right Central executive network, DAN: Dorsal attention network, medVN: medial visual network, lateral VN: lateral visual network, priVN: primary visual network, SMN: Sensorimotor network, BGCN: Basal ganglia and cerebellar network. The results that showed significant correlations with both tasks were indicated by [a].

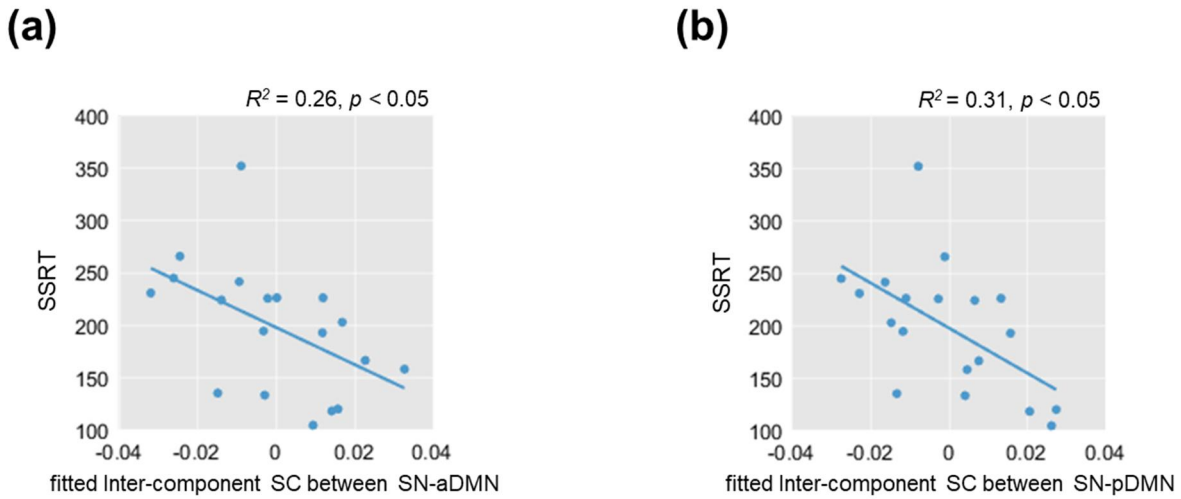

Figure 10. Significant correlations between inter-component structural connectivity (SC) and response inhibition. The higher mean fractional anisotropy (FA) of reconstructed streamlines connecting (a) SN-aDMN (R^2 = 0.26, p < 0.05) and (b) SN-pDMN (R^2 = 0.31, p < 0.05) was associated with better performance of SST.

.

Table 6. The results that showed significant correlations between inter-component structural connectivity and behavioral tasks.

Variable (Task)	Pair of components	*r*	*p*-value (uncorrected)
SSRT			
	SN-aDMN	-0.51	< 0.05
	SN-pDMN	-0.56	< 0.05

SSRT: Strop-signal reaction time, aDMN: anterior default mode network, pDMN: posterior DMN, SN: Salience network.

3.4. Relationship between functional connectivity and structural connectivity

In order to provide a deeper understanding of functional connectivity, the relationship between the functional connectivity and the structural connectivity was examined. The connectivity between SN and pDMN was targeted because both functional and structural connectivity showed significant correlations with SSRT. The inter-component functional connectivity and the inter-component structural connectivity between SN and pDMN showed significant negative correlation (r = -0.79, $p < 0.0005$, uncorrected) (Figure 11).

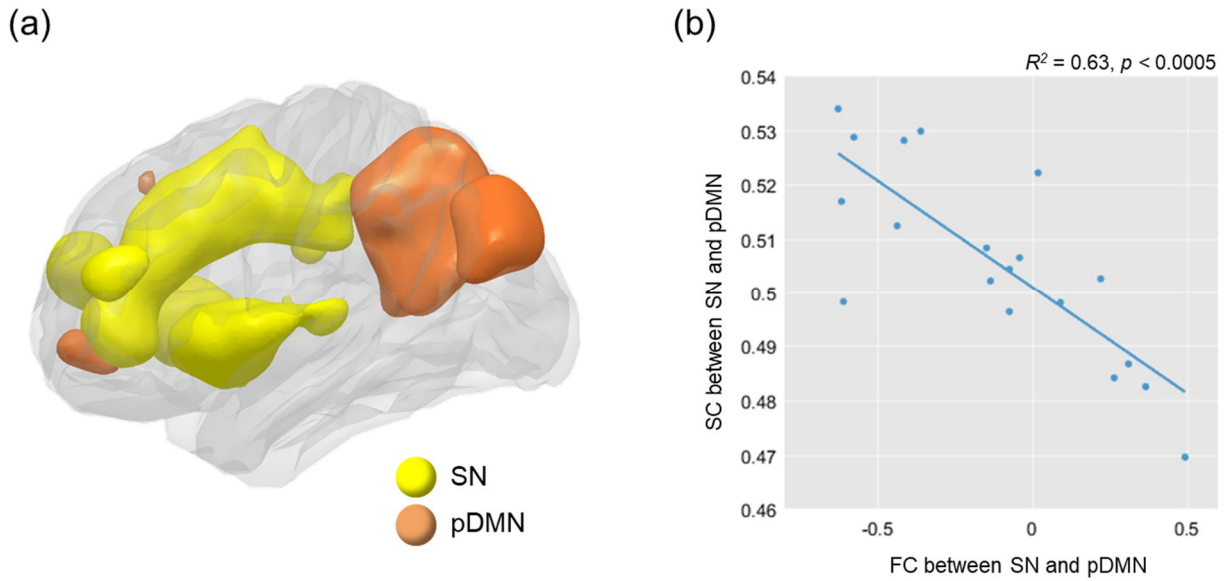

Figure 11. The correlation between functional and structural connectivity of SN-pDMN. (a) SN and pDMN was displayed in yellow and orange, respectively. (b) A significant negative correlation between functional and structural connectivity between SN and pDMN was found (R^2 = 0.63, p < 0.0005, uncorrected).

3.5. Minimum spanning tree

The MSTs of a subject with the best performance on response inhibition and one with the worst were estimated. An MST of the subject with the best performance showed direct connections between SN and aDMN, and between SN and pDMN (Figure 12 (a)). There was no direct connection found in subject with the worst performance (Figure 12 (b), bottom). When MST of all subjects was listed in order of good performance, no direct connection between SN and aDMN/pDMN was found in the bottom seven subjects (Figure 13).

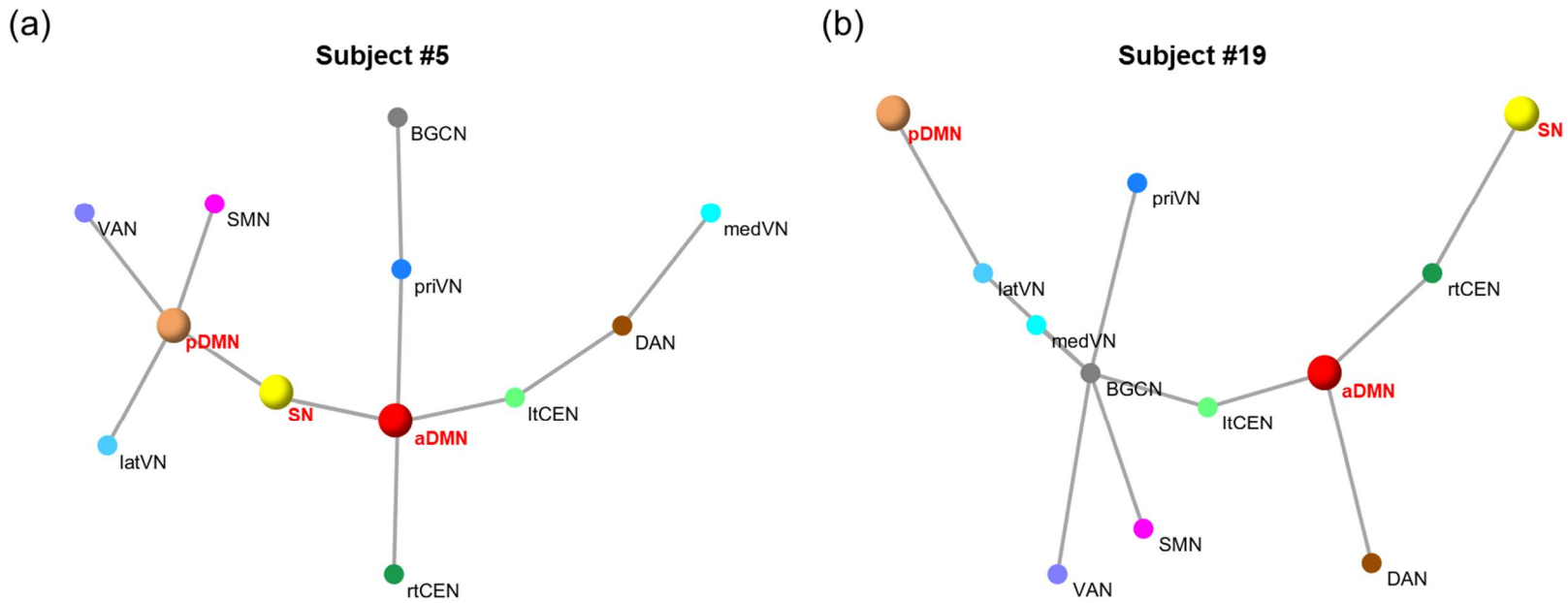

Figure 12. Minimum spanning tree (MST) of the best and the worst performers. The MST estimated from a subject whose performances were the best (a) and the worst (b).

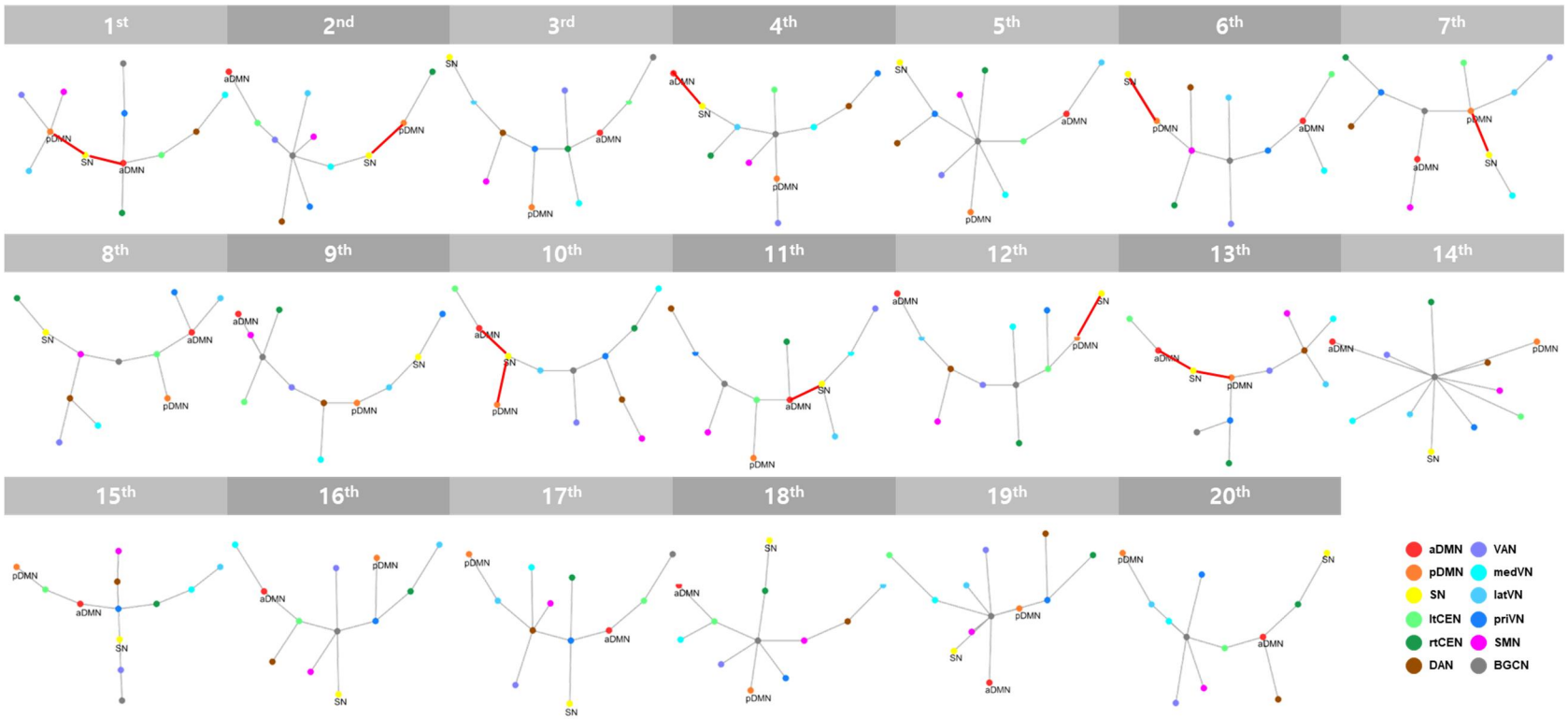

Figure 13. The minimum spanning trees of all subjects. The minimum spanning trees of all subjects were listed in order of good performance, considering both tasks. The red line represents a direct connection between SN and aDMN and between SN and pDMN.

4. Discussion

The converging evidence indicated that the connectivity within SN and between SN and DMN components are the critical indicators of individual differences in response inhibition. The stronger structural connectivity and lower functional connectivity at rest of SN were related to better response inhibition. Greater structural connectivity and greater anti-correlation between SN and DMN components were associated with better response inhibition.

4.1. Resting-state network and cognition

The healthy brain suppresses task-positive networks and activates DMN at rest (Gusnard et al., 2001). In contrast, DMN is suppressed, and task-positive networks are activated during the task (Raichle et al., 2001; Sambataro et al., 2010). Therefore, the anti-correlated nature between DMN and task-positive networks were consistently demonstrated during a task and at rest (Fox et al., 2005; Kelly et al., 2008).

The brain with deficit showed abnormal activation or abnormal functional connectivity of large-scale networks in previous studies. The patients with schizophrenia showed increased functional connectivity within DMN and reduced anti-correlation between DMN and CEN in both resting-state and during the task (Whitfield-Gabrieli et al., 2009). Reduced anti-correlation between DMN and SN was also reported in patients with schizophrenia (Chai

et al., 2011) and bipolar disorders (Lopez-Larson et al., 2017). It implies that abnormal functional connectivity at rest or during a task is associated with cognitive impairment. In healthy adults, sleep deprivation resulted in poor task performance and reduced anti-correlation between DMN and insula in both resting-state and during the task (De Havas et al., 2012). In addition, the magnitude of anti-correlation between DMN and task-positive networks shows robust growth as age increases in healthy subjects age 8-24 years (Chai et al., 2014).

In total, previous studies found that the abnormal connectivity within a large-scale network or reduced anti-correlation between DMN and task-positive networks were related to a deficit of cognitive function. It underpins that a poorly attuned brain may lead to unsuccessful cognitive processing or even impairments of mental states. In particular, SN is one of the most critical component for information processing. Information is abundant around, and an individual has to direct attention to proper information; it can be predators, food, or a word written on the book. In this study, higher functional connectivity within SN and one between SN and DMN, implying cognitive engagement at rest, may lead to inefficient cognitive processes during the task.

4.2. Salience network and response inhibition

The results showed that subjects with stronger intra-component functional connectivity in SN, sensorimotor, visual, and attention networks show relatively poor response inhibition. Notably, SN revealed significant

relationships with both tasks, and intra-component structural connectivity of SN also showed a significant negative correlation with SSRT. It implies that high white matter integration within SN leads to better response inhibition. However, higher functional connectivity within SN at rest may indicate an inefficient and not optimized operation of SN that induces poor response inhibition during task-induced state.

SN detects the salience stimulus and switches between other resting-state networks to recruit attention and other proper cognitive functions (Fox et al., 2005; Menon, 2015; Menon et al., 2010). SN enables individuals to navigate the environment successfully and reach goals (Uddin, 2016). The core nodes of SN includes aINS and dorsal anterior cingulate cortex (dACC) that are crucial to detect a salient event. The aINS integrates interoceptive and exteroceptive signals from cortical and subcortical regions for a further cognitive process (Craig, 2010; Sterzer et al., 2010). It is known to be involved in information processing, including sensory, motor, emotion, and attention. Task-based functional fMRI studies reported the engagement of aINS in detecting salient stimulus and error awareness (Klein et al., 2007; Menon et al., 2010). Previous studies showed dACC's involvement in control-demanding tasks and error monitoring (Carter et al., 1998; Shackman et al., 2011). Not only each node of SN separately, but their connectivity together was also investigated since they are functionally and structurally connected (Allman et al., 2010; Menon, 2011). Not only at rest but also during a task, aINS and dACC showed co-activation, which suggests they work together as a core task-set system (Dosenbach et al., 2006; Engstrom et al., 2013).

Some studies found that increased functional connectivity of SN at rest is related to psychiatric disorders. The hyper-connectivity within SN was found in ASD children and considered as a distinguishing feature for classification (Uddin et al., 2013). The subjects with cocaine addiction showed hyper-connectivity within SN (Janes et al., 2018). Furthermore, the patients noted above share maladaptive behaviors associated with cognitive control impairment (Baler et al., 2006; Poljac et al., 2012). Hyperarousal that induces a hypervigilant stance is the primary symptom of posttraumatic stress disorder (PTSD), and increased functional connectivity within SN was found (Sripada et al., 2012; Uddin et al., 2013). It may imply that hyper-connectivity within the salience network facilitates in detecting a stimulus that might be potentially false, which results in a false alarm. In the same manner, subjects with increased intra-component functional connectivity of SN, which may suggest hypervigilant stance at rest, performed poor response inhibition. Previous studies found that higher expectancy of salient stimulus is related to higher functional connectivity between brain regions in SN during visual cue task (Li et al., 2017). High functional connectivity of SN at rest may reflect the less proficient switching between task-induced state and resting-state, which can lead to poor response inhibition.

The stronger structural connectivity within SN was related to better response inhibition in this study. Previous studies reported that the structural connectivity of SN is associated with the activation or functional connectivity of other large-scale networks, including DMN. A study of traumatic brain injury (TBI) patients demonstrated that white matter integrity of SN predicts DMN

deactivation during a response inhibition task (Bonnelle et al., 2012). The patient who has poor structural connectivity on SN showed failure in DMN deactivation during the task. The damage of the SN tract is related to impairments of the functional coupling between SN and DMN (Jilka et al., 2014), which is considered to be critical to cognitive control (Kelly et al., 2008).

In total, the high structural connectivity and low functional connectivity within SN when there are no cognitive demands may be indicators of proficient and optimized operation for response inhibition. The stronger structural connectivity of SN was related to better response inhibition in this study. The structural connectivity may underlie functional connectivity during the task, and the low functional connectivity at rest may indicate the ability to modulate functional connectivity with the cognitive demands. However, the task-based analysis was not conducted in this analysis, so further research, with fMRI data at rest and during the task, and DTI data together, is required.

4.3. Connectivity between SN and DMN

4.3.1. Functional connectivity between SN and DMN

It was found that connectivity between SN and aDMN/pDMN showed significant associations with response inhibition in both functional and structural modalities. Functional and topological data analysis suggested the importance of anti-correlation between SN and DMN components. The greater anti-correlation of SN-DMN components were related to better response

inhibition. Subjects with higher structural connectivity between SN and DMN components showed better response inhibition and also greater anti-correlation. The MST of a subject with the best response inhibition showed the direct connections between SN and DMN components, whereas the bottom seven subjects including one with the poorest response inhibition performance do not.

Previous studies suggested the nature of anti-correlation between DMN and task-positive networks, and it is crucial for the control-demanding cognitive process (Fox et al., 2005; Fransson, 2005). The greater magnitude of anti-correlation between SN and DMN was related to more successful performance in healthy adults (Kelly et al., 2008; Putcha et al., 2016). The brain has functionally segregated networks, and resting-state networks that internally oriented have opposing and competitive relationships to ones that externally oriented. DMN is involved in an internally focused task, including autobiographical memory, mind wandering, and theory of mind (Buckner et al., 2008). Since DMN manages the self-referential process, SN that directs attention to the stimulus and cognitive processing suppresses DMN during the cognitive tasks. SN deactivates and DMN activates when there is no stimulus given. Based on studies that demonstrated lack of DMN suppression is related to cognitive deficits (Whitfield-Gabrieli et al., 2009; Zhou et al., 2016), the failure of SN to suppress DMN may induce unsuccessful response inhibition.

4.3.2. Structural connectivity between SN and DMN

Structural connectivity is also crucial to understand the nature of neural

circuitry. Previous studies have implicated that white matter structural architectures may underlie large-scale networks (Van Den Heuvel et al., 2009). For example, not only functional connectivity but also structural connectivity showed right-sided laterality within SN (Zhang et al., 2019), and it suggests a close relationship between function and structure of resting-state networks.

In this study, connectivity between SN and pDMN showed a positive correlation in functional analysis and a negative correlation in structural analysis with SSRT. Moreover, the relationship between functional and structural connectivity of SN-pDMN was found: the stronger the anatomical pathway connected, the stronger anti-correlation. The results suggest that there may exist a direct anatomical pathway connecting SN and DMN that plays an important role for SN to modulate DMN.

Previous studies imply that structural connectivity related to SN is associated with response inhibition. In particular, researchers found that the structural integrity of SN was related to the performance of response inhibition (Bonnelle et al., 2012; Xing et al., 2014).

In a previous study, stronger anti-correlation between SN and DMN during the task was correlated with both greater task-induced deactivation in DMN during a task and lower glutamate/GABA ratio PCC and precuneus (Gu et al., 2019). Furthermore, functional interaction between DMN-SN partially mediated the relationship between task-induced deactivation in DMN and glutamate/GABA ratio of PCC/precuneus. It suggests that anti-correlation between SN and DMN may be induced by GABAergic interneurons that send signals from SN to DMN to suppress DMN. The negative correlation between

functional and structural connectivity between SN and pDMN in this study may suggest that the more interneurons from SN that suppress the activation of DMN during the task, the better response inhibition performance.

This study underpins the importance of structural connectivity for both functional connectivity and cognitive function. However, it remains unclear whether the GABAergic interneurons induce the anti-correlation, and further research is needed.

4.3.3. Topological characteristics between SN and DMN

The direct connections between SN and DMN components were found in MST of the best performer, while no direct connection was found in MST of the worst performer. There were no direct connections in MSTs of the bottom seven performers when all MST was shown. The MST also showed that the greater anti-correlation between SN and DMN is still important when whole components are considered as a single connected system. MST represents the most efficient backbone structure since it has the minimum cost. A direct connection represents a robust competitive relationship over limited computational resources between SN and DMN components. It reflects an individual's ability to allocate resources for given cognitive demands: allocate resources to SN to enter and maintain task-induced state, and to DMN to stay at rest (Kucyi et al., 2018; Sonuga-Barke et al., 2007).

In recent studies, topological characteristics that illustrate the hidden features of the brain networks became one of the major methods in

neuroscience. The study that investigated topological characteristics showed superior performance in the classification of clinical samples compared to network measures. The functional connectivity using fluorodeoxyglucose-positron emission tomography data was used to calculate single linkage distance (Lee et al., 2011a), and the single linkage distance demonstrated unique attributes of typical developing and developmental disorders (Ha et al., 2020; Lee et al., 2011a). The topological analysis also showed frontal lobe alterations of the functional connectome in ADHD (Gracia-Tabuenca et al., 2020).

In this study, a direct edge between SN and DMN was found in a subject with superior performance, which is consistent with inter-component functional connectivity analysis. However, the analysis using MST was not statistically tested.

4.4. Limitations of the study

This study has some limitations to be acknowledged. First, the sample size is relatively small, and it is not sufficient to generalize the results. Besides, the sample exhibits gender bias, so it was statistically regressed out. In particular, the gender effect on response inhibition tasks and psychiatric disorders have been consistently reported (Fillmore et al., 2004; Li et al., 2006; Rubia et al., 2013). In this study, no gender difference was found in the connectivity of SN and SN-DMN, but sampling bias can lead to an underestimation of the gender effect. Second, this study did not perform a correction for multiple comparisons,

which may induce false positives. Instead, this study focused on results that are consistently found in both SST and the Stroop task. Both two tasks measure the common underlying mechanisms, the response inhibition, and this approach may enable the investigation of response inhibition without task-specific effect. Third, the independence of the subject-specific IC estimated using dual regression is not optimized and guaranteed. Group ICA approaches to generate a single group IC map, which enables the correspondence of IC maps across subjects. It has been noted the independence is optimized at the group level, but not the subject level (Du et al., 2013; Du et al., 2015). The functional connectivity between components of the subject-level may be a byproduct of the dependence remained at the subject level.

5. Conclusion

In this study, it was aimed to reveal the heterogeneity in large-scale network characteristics that underlies individual variances of response inhibition. It was found that the functinoal connectivity and structrual connectivity at rest within SN and between SN and DMN were associated with the performance of response inhibition. The results imply that higher structural connectivity within SN and between SN and DMN is required for better response inhibition. However, functionally higher connectivity within SN and between SN and DMN at rest may be the indicatives of inefficient modulation, which results in poor response inhibition. The study might suggest that the connectivity of large-scale networks with no task condition can be the indicator of cognitive processing. The results extend our understanding of how large-scale networks at rest contribute to cognition.

References

Allman, J. M., Tetreault, N. A., Hakeem, A. Y., Manaye, K. F., Semendeferi, K., Erwin, J. M., Park, S., Goubert, V., & Hof, P. R. (2010). The von Economo neurons in frontoinsular and anterior cingulate cortex in great apes and humans. *Brain Structure and Function, 214*(5-6), 495-517.

Amer, T., Anderson, J. A., Campbell, K. L., Hasher, L., & Grady, C. L. (2016). Age differences in the neural correlates of distraction regulation: A network interaction approach. *NeuroImage, 139*, 231-239.

Andersson, J. L., & Sotiropoulos, S. N. (2016). An integrated approach to correction for off-resonance effects and subject movement in diffusion MR imaging. *NeuroImage, 125*, 1063-1078.

Aron, A. R. (2007). The neural basis of inhibition in cognitive control. *The Neuroscientist, 13*(3), 214-228.

Aron, A. R., Fletcher, P. C., Bullmore, E. T., Sahakian, B. J., & Robbins, T. W. (2003). Stop-signal inhibition disrupted by damage to right inferior frontal gyrus in humans. *Nature Neuroscience, 6*(2), 115-116.

Aron, A. R., & Poldrack, R. A. (2006). Cortical and subcortical contributions to stop signal response inhibition: role of the subthalamic nucleus. *Journal of Neuroscience, 26*(9), 2424-2433.

Aron, A. R., Robbins, T. W., & Poldrack, R. A. (2004). Inhibition and the right inferior frontal cortex. *Trends in Cognitive Sciences, 8*(4), 170-177.

Aron, A. R., Robbins, T. W., & Poldrack, R. A. (2014). Inhibition and the right inferior frontal cortex: one decade on. *Trends in Cognitive Sciences, 18*(4), 177-185.

Baler, R. D., & Volkow, N. D. (2006). Drug addiction: the neurobiology of disrupted self-control. *Trends in Molecular Medicine, 12*(12), 559-566.

Barber, A. D., Caffo, B. S., Pekar, J. J., & Mostofsky, S. H. (2013). Developmental changes in within-and between-network connectivity between late childhood and adulthood. *Neuropsychologia, 51*(1), 156-167.

Bechara, A., & Martin, E. M. (2004). Impaired decision making related to

working memory deficits in individuals with substance addictions. *Neuropsychology, 18*(1), 152.

Beckmann, C. F., Mackay, C. E., Filippini, N., & Smith, S. M. (2009). Group comparison of resting-state FMRI data using multi-subject ICA and dual regression. *NeuroImage, 47*(Suppl 1), S148.

Bennett, C. M., & Miller, M. B. (2013). fMRI reliability: influences of task and experimental design. *Cognitive, Affective, & Behavioral Neuroscience, 13*(4), 690-702.

Bonnelle, V., Ham, T. E., Leech, R., Kinnunen, K. M., Mehta, M. A., Greenwood, R. J., & Sharp, D. J. (2012). Salience network integrity predicts default mode network function after traumatic brain injury. *Proceedings of the National Academy of Sciences, 109*(12), 4690-4695.

Buckner, R. L., Andrews-Hanna, J. R., & Schacter, D. L. (2008). The brain's default network: anatomy, function, and relevance to disease.

Bullmore, E., & Sporns, O. (2012). The economy of brain network organization. *Nature Reviews Neuroscience, 13*(5), 336-349.

Bunge, S. A., Dudukovic, N. M., Thomason, M. E., Vaidya, C. J., & Gabrieli, J. D. (2002). Immature frontal lobe contributions to cognitive control in children: evidence from fMRI. *Neuron, 33*(2), 301-311.

Carter, C. S., Braver, T. S., Barch, D. M., Botvinick, M. M., Noll, D., & Cohen, J. D. (1998). Anterior cingulate cortex, error detection, and the online monitoring of performance. *Science, 280*(5364), 747-749.

Chai, X. J., Ofen, N., Gabrieli, J. D., & Whitfield-Gabrieli, S. (2014). Selective development of anticorrelated networks in the intrinsic functional organization of the human brain. *Journal of Cognitive Neuroscience, 26*(3), 501-513.

Chai, X. J., Whitfield-Gabrieli, S., Shinn, A. K., Gabrieli, J. D., Castanón, A. N., McCarthy, J. M., Cohen, B. M., & Öngür, D. (2011). Abnormal medial prefrontal cortex resting-state connectivity in bipolar disorder and schizophrenia. *Neuropsychopharmacology, 36*(10), 2009-2017.

Chikazoe, J., Konishi, S., Asari, T., Jimura, K., & Miyashita, Y. (2007). Activation of right inferior frontal gyrus during response inhibition

across response modalities. *Journal of Cognitive Neuroscience, 19*(1), 69-80.

Conturo, T. E., Lori, N. F., Cull, T. S., Akbudak, E., Snyder, A. Z., Shimony, J. S., McKinstry, R. C., Burton, H., & Raichle, M. E. (1999). Tracking neuronal fiber pathways in the living human brain. *Proceedings of the National Academy of Sciences, 96*(18), 10422-10427.

Craig, A. (2010). The sentient self. *Brain Structure and Function, 214*, 563-577.

Damoiseaux, J. S., Rombouts, S., Barkhof, F., Scheltens, P., Stam, C. J., Smith, S. M., & Beckmann, C. F. (2006). Consistent resting-state networks across healthy subjects. *Proceedings of the National Academy of Sciences, 103*(37), 13848-13853.

De Havas, J. A., Parimal, S., Soon, C. S., & Chee, M. W. (2012). Sleep deprivation reduces default mode network connectivity and anti-correlation during rest and task performance. *NeuroImage, 59*(2), 1745-1751.

Di, X., & Biswal, B. B. (2014). Modulatory interactions between the default mode network and task positive networks in resting-state. *PeerJ, 2*, e367.

Dosenbach, N. U., Visscher, K. M., Palmer, E. D., Miezin, F. M., Wenger, K. K., Kang, H. C., Burgund, E. D., Grimes, A. L., Schlaggar, B. L., & Petersen, S. E. (2006). A core system for the implementation of task sets. *Neuron, 50*(5), 799-812.

Douaud, G., & Turner, M. (2015). The Role of Neuroimaging in Amyotrophic Lateral Sclerosis. *Brain Mapping*, 787-797

Du, Y., & Fan, Y. (2013). Group information guided ICA for fMRI data analysis. *NeuroImage, 69*, 157-197.

Du, Y., Pearlson, G. D., Liu, J., Sui, J., Yu, Q., He, H., Castro, E., & Calhoun, V. D. (2015). A group ICA based framework for evaluating resting fMRI markers when disease categories are unclear: application to schizophrenia, bipolar, and schizoaffective disorders. *NeuroImage, 122*, 272-280.

Elman, J. A., Madison, C. M., Baker, S. L., Vogel, J. W., Marks, S. M., Crowley,

S., O'neil, J. P., & Jagust, W. J. (2014). Effects of beta-amyloid on resting state functional connectivity within and between networks reflect known patterns of regional vulnerability. *Cerebral Cortex, 26*(2), 695-707.

Engstrom, M., Landtblom, A.-M., & Karlsson, T. (2013). Brain and effort: brain activation and effort-related working memory in healthy participants and patients with working memory deficits. *Frontiers in Human Neuroscience, 7*, 140.

Erika-Florence, M., Leech, R., & Hampshire, A. (2014). A functional network perspective on response inhibition and attentional control. *Nature Communications, 5*, 4073.

Fichten, C. S., & Bourdon, C. V. (1986). Social skill deficit or response inhibition: Interaction between disabled and nondisabled college students. *Journal of College Student Personnel, 27*(4), 326-333.

Filippini, N., MacIntosh, B. J., Hough, M. G., Goodwin, G. M., Frisoni, G. B., Smith, S. M., Matthews, P. M., Beckmann, C. F., & Mackay, C. E. (2009). Distinct patterns of brain activity in young carriers of the APOE-ε4 allele. *Proceedings of the National Academy of Sciences, 106*(17), 7209-7214.

Fillmore, M. T., & Weafer, J. (2004). Alcohol impairment of behavior in men and women. *Addiction, 99*(10), 1237-1246.

Fox, M. D., & Greicius, M. (2010). Clinical applications of resting state functional connectivity. *Frontiers in Systems Neuroscience, 4*, 19.

Fox, M. D., Snyder, A. Z., Vincent, J. L., Corbetta, M., Van Essen, D. C., & Raichle, M. E. (2005). The human brain is intrinsically organized into dynamic, anticorrelated functional networks. *Proceedings of the National Academy of Sciences, 102*(27), 9673-9678.

Fransson, P. (2005). Spontaneous low-frequency BOLD signal fluctuations: An fMRI investigation of the resting-state default mode of brain function hypothesis. *Human Brain Mapping, 26*(1), 15-29.

Friedman, N. P., & Miyake, A. (2004). The relations among inhibition and interference control functions: a latent-variable analysis. *Journal of*

Experimental Psychology: General, 133(1), 101.

Gauggel, S., Rieger, M., & Feghoff, T. (2004). Inhibition of ongoing responses in patients with Parkinson's disease. *Journal of Neurology, Neurosurgery & Psychiatry, 75*(4), 539-544.

Gielen, J., Wiels, W., Van Schependom, J., Laton, J., Van Hecke, W., Parizel, P. M., D'hooghe, M. B., & Nagels, G. (2018). The effect of task modality and stimulus frequency in paced serial addition tests on functional brain activity. *PLoS One, 13*(3), e0194388.

Giusti, C., Ghrist, R., & Bassett, D. S. (2016). Two's company, three (or more) is a simplex. *Journal of Computational Neuroscience, 41*(1), 1-14.

Gracia-Tabuenca, Z., Díaz-Patiño, J. C., Arelio, I., & Alcauter, S. (2020). Topological Data Analysis reveals robust alterations in the whole-brain and frontal lobe functional connectomes in Attention-Deficit/Hyperactivity Disorder. *eNeuro*.

Gu, H., Hu, Y., Chen, X., He, Y., & Yang, Y. (2019). Regional excitation-inhibition balance predicts default-mode network deactivation via functional connectivity. *NeuroImage, 185*, 388-397.

Gusnard, D. A., Akbudak, E., Shulman, G. L., & Raichle, M. E. (2001). Medial prefrontal cortex and self-referential mental activity: relation to a default mode of brain function. *Proceedings of the National Academy of Sciences, 98*(7), 4259-4264.

Ha, S., Lee, H., Choi, Y., Kang, H., Jeon, S. J., Ryu, J. H., Kim, H. J., Cheong, J. H., Lim, S., & Kim, B.-N. (2020). Maturational delay and asymmetric information flow of brain connectivity in SHR model of ADHD revealed by topological analysis of metabolic networks. *Scientific Reports, 10*(1), 1-13.

Hahn, H. (1982). A standardization study of Beck Depression Inventory in Korea. *J Korean Neuropsychiatr Asso, 25*, 487-502.

Hampshire, A., & Sharp, D. J. (2015). Contrasting network and modular perspectives on inhibitory control. *Trends in Cognitive Sciences, 19*(8), 445-452.

Honey, C., Sporns, O., Cammoun, L., Gigandet, X., Thiran, J.-P., Meuli, R., &

Hagmann, P. (2009). Predicting human resting-state functional connectivity from structural connectivity. *Proceedings of the National Academy of Sciences, 106*(6), 2035-2040.

Janes, A., Gilman, J., Frederick, B., Radoman, M., Pachas, G., Fava, M., & Evins, A. (2018). Salience network coupling is linked to both tobacco smoking and symptoms of attention deficit hyperactivity disorder (ADHD). *Drug and Alcohol Dependence, 182*, 93-97.

Jilka, S. R., Scott, G., Ham, T., Pickering, A., Bonnelle, V., Braga, R. M., Leech, R., & Sharp, D. J. (2014). Damage to the salience network and interactions with the default mode network. *Journal of Neuroscience, 34*(33), 10798-10807.

Jones, D. K. (2010). Diffusion mri: *Oxford University Press*.

Kang, Y., Na, D. L., & Hahn, S. (1997). A validity study on the Korean Mini-Mental State Examination (K-MMSE) in dementia patients. *J Korean Neurol Assoc, 15*(2), 300.

Keller, J. B., Hedden, T., Thompson, T. W., Anteraper, S. A., Gabrieli, J. D., & Whitfield-Gabrieli, S. (2015). Resting-state anticorrelations between medial and lateral prefrontal cortex: association with working memory, aging, and individual differences. *Cortex, 64*, 271-280.

Kelly, A. C., Uddin, L. Q., Biswal, B. B., Castellanos, F. X., & Milham, M. P. (2008). Competition between functional brain networks mediates behavioral variability. *NeuroImage, 39*(1), 527-537.

Kim, J., Shin, D., KIM, J., Kim, J., Shin, D., Kim, J., & Shin, G. (1978). A study based on the standardization of the STAI for Korea. *New Med J*, *21*(11), 69-75.

Klein, T. A., Endrass, T., Kathmann, N., Neumann, J., von Cramon, D. Y., & Ullsperger, M. (2007). Neural correlates of error awareness. *NeuroImage, 34*(4), 1774-1781.

Koch, M. A., Norris, D. G., & Hund-Georgiadis, M. (2002). An investigation of functional and anatomical connectivity using magnetic resonance imaging. *NeuroImage, 16*(1), 241-250.

Kong, R., Li, J., Orban, C., Sabuncu, M. R., Liu, H., Schaefer, A., Sun, N., Zuo,

X.-N., Holmes, A. J., & Eickhoff, S. B. (2019). Spatial topography of individual-specific cortical networks predicts human cognition, personality, and emotion. *Cerebral Cortex, 29*(6), 2533-2551.

Kruskal, J. B. (1956). On the shortest spanning subtree of a graph and the traveling salesman problem. *Proceedings of the American Mathematical society, 7*(1), 48-50.

Kucyi, A., Daitch, A., Raccah, O., Zhao, B., Zhang, C., Esterman, M., Zeineh, M., Halpern, C. H., Zhang, K., & Zhang, J. (2018). Anticorrelated inter-network electrophysiological activity varies dynamically with attentional performance and behavioral states. *BioRxiv*, 503193.

Lawrence, A. J., Luty, J., Bogdan, N. A., Sahakian, B. J., & Clark, L. (2009). Impulsivity and response inhibition in alcohol dependence and problem gambling. *Psychopharmacology, 207*(1), 163-172.

Lee, H., Chung, M. K., Choi, H., Kang, H., Ha, S., Kim, Y. K., & Lee, D. S. (2019). Harmonic holes as the submodules of brain network and network dissimilarity. *Paper presented at the International Workshop on Computational Topology in Image Context*. (pp. 110-122). Springer, Cham.

Lee, H., Chung, M. K., Kang, H., Kim, B.-N., & Lee, D. S. (2011a). Computing the shape of brain networks using graph filtration and Gromov-Hausdorff metric. *Paper presented at the International Conference on Medical Image Computing and Computer-Assisted Intervention*. Springer, Berlin, Heidelberg, 2011.

Lee, H., Chung, M. K., Kang, H., Kim, B.-N., & Lee, D. S. (2011b). Discriminative persistent homology of brain networks. *Paper presented at the 2011 IEEE International Symposium on Biomedical Imaging: From Nano to Macro*. (pp. 841-844). IEEE.

Lee, H. W., Lo, Y.-H., Li, K.-H., Sung, W.-S., & Juan, C.-H. (2015). The relationship between the development of response inhibition and intelligence in preschool children. *Frontiers in Psychology, 6*, 802.

Li, C.-s. R., Huang, C., Constable, R. T., & Sinha, R. (2006). Gender differences in the neural correlates of response inhibition during a stop signal task.

NeuroImage, 32(4), 1918-1929.

Li, S., Demenescu, L. R., Sweeney-Reed, C. M., Krause, A. L., Metzger, C. D., & Walter, M. (2017). Novelty seeking and reward dependence-related large-scale brain networks functional connectivity variation during salience expectancy. *Human Brain Mapping, 38*(8), 4064-4077.

Logan, G. D., & Cowan, W. B. (1984). On the ability to inhibit thought and action: A theory of an act of control. *Psychological Review, 91*(3), 295.

Lopez-Larson, M. P., Shah, L. M., Weeks, H. R., King, J. B., Mallik, A. K., Yurgelun-Todd, D. A., & Anderson, J. S. (2017). Abnormal functional connectivity between default and salience networks in pediatric bipolar disorder. *Biological Psychiatry: Cognitive Neuroscience and Neuroimaging, 2*(1), 85-93.

MacLeod, C. M., & MacDonald, P. A. (2000). Interdimensional interference in the Stroop effect: Uncovering the cognitive and neural anatomy of attention. *Trends in Cognitive Sciences, 4*(10), 383-391.

Mazaika, P. K., Whitfield, S., & Cooper, J. C. (2005). Detection and repair of transient artifacts in fMRI data. *NeuroImage, 26*(Suppl 1), S36.

Mckiernan, K. A., Kaufman, J. N., Kucera-Thompson, J., & Binder, J. R. (2003). A parametric manipulation of factors affecting task-induced deactivation in functional neuroimaging. *Journal of Cognitive Neuroscience, 15*(3), 394-408.

Menon, V. (2011). Large-scale brain networks and psychopathology: a unifying triple network model. *Trends in Cognitive Sciences, 15*(10), 483-506.

Menon, V. (2015). Salience network.

Menon, V., & Uddin, L. Q. (2010). Saliency, switching, attention and control: a network model of insula function. *Brain Structure and Function, 214*(5-6), 655-667.

Mori, S., Crain, B. J., Chacko, V. P., & Van Zijl, P. C. (1999). Three-dimensional tracking of axonal projections in the brain by magnetic resonance imaging. *Annals of Neurology: Official Journal of the American Neurological Association and the Child Neurology Society, 45*(2), 265-269.

Nigg, J. T., Wong, M. M., Martel, M. M., Jester, J. M., Puttler, L. I., Glass, J. M., Adams, K. M., Fitzgerald, H. E., & Zucker, R. A. (2006). Poor response inhibition as a predictor of problem drinking and illicit drug use in adolescents at risk for alcoholism and other substance use disorders. *Journal of the American Academy of Child & Adolescent Psychiatry, 45*(4), 468-475.

Nour, M. M., Dahoun, T., McCutcheon, R. A., Adams, R. A., Wall, M. B., & Howes, O. D. (2019). Task-induced functional brain connectivity mediates the relationship between striatal D2/3 receptors and working memory. *Elife, 8*, e45045.

Olson, I. R., Von Der Heide, R. J., Alm, K. H., & Vyas, G. (2015). Development of the uncinate fasciculus: Implications for theory and developmental disorders. *Developmental Cognitive Neuroscience, 14*, 50-61.

Patel, A. X., & Bullmore, E. T. (2016). A wavelet-based estimator of the degrees of freedom in denoised fMRI time series for probabilistic testing of functional connectivity and brain graphs. *NeuroImage, 142*, 14-26.

Patel, A. X., Kundu, P., Rubinov, M., Jones, P. S., Vértes, P. E., Ersche, K. D., Suckling, J., & Bullmore, E. T. (2014). A wavelet method for modeling and despiking motion artifacts from resting-state fMRI time series. *NeuroImage, 95*, 287-304.

Poljac, E., & Bekkering, H. (2012). A review of intentional and cognitive control in autism. *Frontiers in Psychology, 3*, 436.

Power, J. D., Barnes, K. A., Snyder, A. Z., Schlaggar, B. L., & Petersen, S. E. (2012). Spurious but systematic correlations in functional connectivity MRI networks arise from subject motion. *NeuroImage, 59*(3), 2142-2154.

Putcha, D., Ross, R. S., Cronin-Golomb, A., Janes, A. C., & Stern, C. E. (2016). Salience and default mode network coupling predicts cognition in aging and Parkinson's disease. *Journal of the International Neuropsychological Society, 22*(2), 205-215.

Raichle, M. E., MacLeod, A. M., Snyder, A. Z., Powers, W. J., Gusnard, D. A., & Shulman, G. L. (2001). A default mode of brain function.

Proceedings of the National Academy of Sciences, 98(2), 676-682.

Roberts, R. J., Hager, L. D., & Heron, C. (1994). Prefrontal cognitive processes: Working memory and inhibition in the antisaccade task. *Journal of Experimental Psychology: General, 123*(4), 374.

Rolinski, M., Griffanti, L., Szewczyk-Krolikowski, K., Menke, R. A., Wilcock, G. K., Filippini, N., Zamboni, G., Hu, M. T., & Mackay, C. E. (2015). Aberrant functional connectivity within the basal ganglia of patients with Parkinson's disease. *NeuroImage: Clinical, 8*, 126-132.

Rollans, C., & Cummine, J. (2018). One tract, two tract, old tract, new tract: A pilot study of the structural and functional differentiation of the inferior fronto-occipital fasciculus. *Journal of Neurolinguistics, 46*, 122-137.

Rubia, K., Lim, L., Ecker, C., Halari, R., Giampietro, V., Simmons, A., Brammer, M., & Smith, A. (2013). Effects of age and gender on neural networks of motor response inhibition: from adolescence to mid-adulthood. *NeuroImage, 83*, 690-703.

Rubia, K., Russell, T., Overmeyer, S., Brammer, M. J., Bullmore, E. T., Sharma, T., Simmons, A., Williams, S. C., Giampietro, V., & Andrew, C. M. (2001). Mapping motor inhibition: conjunctive brain activations across different versions of go/no-go and stop tasks. *NeuroImage, 13*(2), 250-261.

Sala-Llonch, R., Pena-Gomez, C., Arenaza-Urquijo, E. M., Vidal-Piñeiro, D., Bargallo, N., Junque, C., & Bartres-Faz, D. (2012). Brain connectivity during resting state and subsequent working memory task predicts behavioural performance. *Cortex, 48*(9), 1187-1196.

Sambataro, F., Murty, V. P., Callicott, J. H., Tan, H.-Y., Das, S., Weinberger, D. R., & Mattay, V. S. (2010). Age-related alterations in default mode network: impact on working memory performance. *Neurobiology of Aging, 31*(5), 839-852.

Shackman, A. J., Salomons, T. V., Slagter, H. A., Fox, A. S., Winter, J. J., & Davidson, R. J. (2011). The integration of negative affect, pain and cognitive control in the cingulate cortex. *Nature Reviews Neuroscience, 12*(3), 154-167.

Slaats-Willemse, D., Swaab-Barneveld, H., De Sonneville, L., Van Der Meulen, E., & Buitelaar, J. (2003). Deficient response inhibition as a cognitive endophenotype of ADHD. *Journal of the American Academy of Child & Adolescent Psychiatry, 42*(10), 1242-1248.

Sonuga-Barke, E. J., & Castellanos, F. X. (2007). Spontaneous attentional fluctuations in impaired states and pathological conditions: a neurobiological hypothesis. *Neuroscience & Biobehavioral Reviews, 31*(7), 977-986.

Sripada, R. K., King, A. P., Welsh, R. C., Garfinkel, S. N., Wang, X., Sripada, C. S., & Liberzon, I. (2012). Neural dysregulation in posttraumatic stress disorder: evidence for disrupted equilibrium between salience and default mode brain networks. *Psychosomatic Medicine, 74*(9), 904.

Sterzer, P., & Kleinschmidt, A. (2010). Anterior insula activations in perceptual paradigms: often observed but barely understood. *Brain Structure and Function, 214*(5-6), 611-622.

Stroop, J. R. (1935). Studies of interference in serial verbal reactions. *Journal of Experimental Psychology, 18*(6), 643.

Swick, D., Ashley, V., & Turken, U. (2011). Are the neural correlates of stopping and not going identical? Quantitative meta-analysis of two response inhibition tasks. *NeuroImage, 56*(3), 1655-1665.

Thomas Yeo, B., Krienen, F. M., Sepulcre, J., Sabuncu, M. R., Lashkari, D., Hollinshead, M., Roffman, J. L., Smoller, J. W., Zöllei, L., & Polimeni, J. R. (2011). The organization of the human cerebral cortex estimated by intrinsic functional connectivity. *Journal of Neurophysiology, 106*(3), 1125-1165.

Uddin, L. Q. (2016). *Salience network of the human brain*: Academic press.

Uddin, L. Q., Supekar, K., Lynch, C. J., Khouzam, A., Phillips, J., Feinstein, C., Ryali, S., & Menon, V. (2013). Salience network–based classification and prediction of symptom severity in children with autism. *JAMA Psychiatry, 70*(8), 869-879.

Unsworth, N., Miller, J. D., Lakey, C. E., Young, D. L., Meeks, J. T., Campbell, W. K., & Goodie, A. S. (2009). Exploring the relations among

executive functions, fluid intelligence, and personality. *Journal of Individual Differences, 30*(4), 194-200.

van den Heuvel, M., Mandl, R., Luigjes, J., & Pol, H. H. (2008). Microstructural organization of the cingulum tract and the level of default mode functional connectivity. *Journal of Neuroscience, 28*(43), 10844-10851.

Van Den Heuvel, M. P., Mandl, R. C., Kahn, R. S., & Hulshoff Pol, H. E. (2009). Functionally linked resting-state networks reflect the underlying structural connectivity architecture of the human brain. *Human Brain Mapping, 30*(10), 3127-3141.

van der Meer, D.-J., & van der Meere, J. (2004). Response inhibition in children with conduct disorder and borderline intellectual functioning. *Child Neuropsychology, 10*(3), 189-194.

van Duijvenvoorde, A. C., Achterberg, M., Braams, B. R., Peters, S., & Crone, E. A. (2016). Testing a dual-systems model of adolescent brain development using resting-state connectivity analyses. *NeuroImage, 124*, 409-420.

Wang, F., Sun, T., Li, X., Xia, H., & Li, Z. (2011). Microsurgical and tractographic anatomical study of insular and transsylvian transinsular approach. *Neurological Sciences, 32*(5), 865.

Welvaert, M., & Rosseel, Y. (2013). On the definition of signal-to-noise ratio and contrast-to-noise ratio for fMRI data. *PLoS One, 8*(11), e77089.

Wen, X., Liu, Y., Yao, L., & Ding, M. (2013). Top-down regulation of default mode activity in spatial visual attention. *Journal of Neuroscience, 33*(15), 6444-6453.

Whitfield-Gabrieli, S., Thermenos, H. W., Milanovic, S., Tsuang, M. T., Faraone, S. V., McCarley, R. W., Shenton, M. E., Green, A. I., Nieto-Castanon, A., & LaViolette, P. (2009). Hyperactivity and hyperconnectivity of the default network in schizophrenia and in first-degree relatives of persons with schizophrenia. *Proceedings of the National Academy of Sciences, 106*(4), 1279-1284.

Xing, L., Yuan, K., Bi, Y., Yin, J., Cai, C., Feng, D., Li, Y., Song, M., Wang, H.,

& Yu, D. (2014). Reduced fiber integrity and cognitive control in adolescents with internet gaming disorder. *Brain Research, 1586*, 109-117.

Zhang, R., Geng, X., & Lee, T. M. (2017). Large-scale functional neural network correlates of response inhibition: an fMRI meta-analysis. *Brain Structure and Function, 222*(9), 3973-3990.

Zhang, Y., Suo, X., Ding, H., Liang, M., Yu, C., & Qin, W. (2019). Structural connectivity profile supports laterality of the salience network. *Human Brain Mapping, 40*(18), 5242-5255.

Zhou, L., Pu, W., Wang, J., Liu, H., Wu, G., Liu, C., Mwansisya, T. E., Tao, H., Chen, X., & Huang, X. (2016). Inefficient DMN suppression in schizophrenia patients with impaired cognitive function but not patients with preserved cognitive function. *Scientific Reports, 6*(1), 1-10.

국문 초록

반응 억제의 개인차와 관련한 대규모 휴지기 뇌네트워크의 특성

허영민

서울대학교 대학원

협동과정 인지과학 전공

반응 억제는 가장 주요한 인지 기능 중 하나이며 이상행동을 동반하는 다양한 정신 질환과도 깊은 관련이 있다. 따라서 이와 관련된 신경적 특성을 탐구하는 것은 매우 중요하다. 우리의 뇌는 어떠한 인지 기능을 수행할 때, 작업 관련 영역들을 활성화하고 자기 참조적 처리를 하는 디폴트 모드 네트워크 영역들은 비활성화한다. 휴지기에는 반대로 작업 관련 영역들은 비활성화하고 디폴트 모드 네트워크 영역은 활성화한다. 이처럼 인지 기능을 수행하기 위해서는 상태를 효율적으로 전환하는 것이 중요하다. 현출성 네트워크 (salience network)는 어떠한 과제를 할 때 중요한 자극을 탐지하여 처리하며 또한 디폴트 모드 네트워크의 활성을 억제하기 때문에 상태 간 전환에 핵심적인 역할을 하는 대규모 뇌네트워크이다. 따라서 이와 관련된 연결적 특성이 인지 기능과 밀접한 관련이 있으며, 그러한 특성은 휴지기의 연결성에도 반영되어 있을 것이라 가정하였다. 즉, 본 연구에서는 반응 억제의 개인차를 휴지기 대규모 뇌네트워크들의 특성을 통해 설명할 수 있을 것이며, 특히 현출성 네트워크의 낮은 기능적 연결성, 디폴트 모드 네트워크의 높은 기능적 연결성, 그리고 그 둘 간의 높은 기능적 역 상관 (anti-correlation)이 반응 억제에 우수한 사람들의 특징적인 휴지기 연결성일 것이라 가설을 세웠다.

개인의 반응 억제는 정지 신호 과제와 스트룹 과제를 통해

측정하였으며, 휴지기 대규모 뇌네트워크들의 특성들과 어떠한 상관을 갖는지 알아보았다. 즉, 기능적 뇌네트워크 내의 연결성과 두 뇌네트워크 간 연결성이 과제 수행과 어떠한 상관을 보이는지를 알아보았다. 또한 기능적 연결성에 대한 보다 깊은 이해를 위해 확산 텐서 영상과 트랙토그래피 기법을 사용하여 구조적 연결성과 반응 억제와의 상관을 알아보았다. 반응 억제와 관련된 토폴로지 특성 역시 함께 알아보기 위해 참여자들의 미니멈 스패닝 트리(MST: minimum spanning tree)를 계산하였다.

분석 결과, 현출성 네트워크, 그리고 현출성 네트워크와 디폴트 모드 네트워크 간의 연결성을 통해 반응 억제의 개인차를 설명할 수 있었다. 현출성 네트워크의 성분 내 구조적 연결성은 강하지만 휴지기의 기능적 연결성이 약한 참여자들일수록 반응 억제 수행이 우수했다. 현출성 네트워크와 디폴트 모드 네트워크 간의 구조적 연결성과 기능적 역 상관은 모두 높을수록 우수한 반응 억제를 보였다. 또한 두 네트워크 간 구조적 연결성이 높을수록 기능적 역 상관이 높은 것으로 나타났다. 토폴로지 분석에서는 가장 수행이 좋은 참여자의 MST는 현출성 네트워크와 디폴트 모드 네트워크들 간에 직접적인 연결이 관찰되었으나 수행이 가장 나쁜 참여자에서는 그러한 직접적인 연결이 관찰되지 않았다.

분석 결과, 휴지기의 현출성 네트워크 내 연결성, 그리고 현출성 네트워크와 디폴트 모드 네트워크 간의 기능적 역 상관과 구조적 연결성이 반응 억제의 개인 차이를 설명하였으나, 디폴트 모드 네트워크 내의 연결성은 그렇지 못했다. 이 연구는 과제 수행 중이 아닌 휴지기 동안의 뇌네트워크의 특성들을 통해 반응 억제의 개인차를 설명할 수 있음을 보여준다.

Keywords: 반응 억제, 휴지기 기능적 자기공명영상, 확산 텐서 영상, 대규모 네트워크, 미니멈 스패닝 트리

Student Number: 2014-30038